COMPARING THE CONCENTRATION OF RADON IN THE OLD AND NEW RESIDENTIAL HOUSES IN KARABUK CITY/TURKEY USING THE PASSIVE METHOD

2024
MASTER THESIS
PHYSICS

Abdulrahman Ahmed Mustafa AL-AJILI

Thesis Advisor
Assist. Prof. Dr. Khalid Hadi Mahdi AL-SHABEEB

COMPARING THE CONCENTRATION OF RADON IN THE OLD AND NEW RESIDENTIAL HOUSES IN KARABUK CITY/TURKEY USıNG THE PASSIVE METHOD

Abdulrahman Ahmed Mustafa AL-AJILI

Thesis Advisor
Assist. Prof. Dr. Khalid Hadi Mahdi AL-SHABEEB

T.C.
Karabuk University
Institute of Graduate Program
Department of Physics
Prepared as
Master Thesis

KARABÜK
February 2024

I certify that in my opinion the thesis submitted by Abdulrahman Ahmed Mustafa AL-AJILI titled “COMPARING THE CONCENTRATION OF RADON IN THE OLD AND NEW RESIDENTIAL HOUSES IN KARABUK CITY/TURKEY USING THE PASSIVE METHOD” is fully adequate in scope and in quality as a thesis for the degree of Master Thesis.

Assist. Prof. Dr. Khalid Hadi Mahdi AAL-SHABEEB .....

Thesis Advisor, Department of Physics Department

This thesis is accepted by the examining committee with a unanimous vote in the Department of Physics Department as a Master of Science thesis. 01/02/2024

Examining Committee Members (Institutions)	Signature
Chairman : Assist. Prof. Dr. Khalid AL-SHABEEB (KBU)	.....
Member : Prof. Dr. Aybaba HANÇERLİOĞULLARI (KU)	.....
Member : Assoc. Prof. Dr. Hüseyin YILDIRIM (KBU)	.....

The degree of Master of Science by the thesis submitted is approved by the Administrative Board of the Institute of Graduate Programs, Karabuk University.

Assoc. Prof. Dr. Zeynep ÖZCAN .....

Director of the Institute of Graduate Programs

"*All information in this letter has been obtained and provided by academic rules and ethical principles; I further certify that I have provided all attribution that does not arise in this work, as required by these rules and principles"*

Abdulrahman Ahmed Mustafa AL-AJILI

ABSTRACT

M. Sc. Thesis

COMPARING THE CONCENTRATıON OF RADON IN THE OLD AND NEW RESIDENTIAL HOUSES IN KARABUK CITY/TURKEY USING THE PASSIVE METHOD

Abdulrahman Ahmed Mustafa AL-AJILI

Karabuk University
Institute of Graduate Programs
Department of Physics

Thesis Advisor:
Assist. Prof. Dr. Khalid Hadi Mahdi AL-SHABEEB
February 2024, 81 pages

This study is an update of the little information about Radon concentration available for the Karabuk region, especially the old residential houses. 10 old residential houses and 15 modern houses selected in the summer season, and 10 old and identical new houses in the winter 180 CR-39 track detectors, four for each house, suspended in the living and sleeping rooms for one month. The detectors were then collected and chemically etched. The results indicated that the average radon concentrations in the old houses (with a range of 82.884 to 113.083 Bq/m^3) higher than in the modern ones (with a range of 55.884 to 77.581 Bq/m^3) by 52.78% in the winter season. With 39.78% in the summer season (with a range of 34.845 to 60.487 Bq/m^3) and (with a range of 32.215 to 51.282 Bq/m^3) respectively. This is due to the nature of the building materials used and the construction style (where we find glass facades that occupy larger areas in modern houses). The radioactive levels of radon gas also computed,

revealing higher concentrations in the old dwellings compared to the modern houses. Nevertheless, both values fall below the thresholds advised by scientific authorities such as UNSCEAR and the ICRP.

Keywords **:** CR-39 Detector, Radon, Old Residential Houses.
Science Code **:** 20216

ÖZET

Yüksek Lisans Tezi

KARABÜK İLİ/TÜRKIYE'DEKİ ESKİ VE YENİ KONUTLARDAKİ RADON KONSANTRASYONUNUN PASİF YÖNTEM KULLANILARAK KARŞILAŞTIRILMASI

Abdulrahman Ahmed Mustafa AL-AJILI

Karabük Üniversitesi
Lisansüstü Eğitim Enstitüsü
Fizik Anabilim Dalı

Tez Danışmanı:
Assist. Prof. Dr. Halid Hadi Mehdi AL-SHABEEB
Şubat 2024, 81 Sayfa

Bu çalışma, Karabük bölgesi için mevcut Radon konsantrasyonu hakkında az miktarda bilginin güncellenmesi olup, özellikle eski konutlar, 10 eski konut ve 15 modern ev yaz sezonunda, 10 eski ve aynı yeni ev ise kış sezonunda seçilmiştir. Her eve 4 adet olmak üzere 180 adet CR-T9 takip dedektörü bir ay süreyle oturma ve yatak odalarında asılı kaldı. Daha sonra dedektörler toplandı ve kimyasal olarak aşındırıldı. Sonuçlar, kış mevsiminde eski evlerdeki ortalama radon konsantrasyonunun (82.884 ila 113.083 Bq/m3 aralığında) modern evlere göre (55.884 ila 77.581 Bq/m3 aralığında) %52,78 daha yüksek olduğunu gösterdi. yaz sezonunda ise %39,78 (34.845 ile 60.487 Bq/m3 aralığında) ve (32.215 ile 51.282 Bq/m3 aralığında) şeklindedir. Bunun nedeni, kullanılan yapı malzemelerinin doğasından ve inşaat tarzından kaynaklanmaktadır (modern evlerde daha geniş alanlar kaplayan cam cephelere rastlıyoruz). Radon gazının radyoaktif indeksleri de hesaplandı, yani eski evlerde modern evlere göre daha

yüksekti, ancak her ikisinin de bilimsel kurumların [UNSCEAR & ICRP] önerdiği değerlerden daha düşük olduğunu gördük.

Anahtar Kelimeler **:** CR-39 Dedektörü, Radon, Eski konutlar.
Bilim Kodu **:** 20216

ACKNOWLEDGMENT

To God Almighty, who helped me in my studies, and to our honorable Messenger Muhammad.

I extend my thanks to the university that embraced me, Karbuk University.

I want to extend my sincere thanks and gratitude to Dr. Khaled and all the professors in the physics body who played an effective role in developing my knowledge and understanding in the field of study.

I also extend my thanks to Dr. Abdullah at Tikrit University for helping me.

He thanked my dear family, who supported me during my academic career.

I also thank everyone who helped and stood by me in critical times, especially my friends.

CONTENTS

Page

Page

Page

LIST OF FIGURES

Page

Page

Page

LIST OF TABLES

Page

ABBREVITIONS INDEX

UNSCEAR	: United Nation Scientific Committee on the Effect of Atomic Radiation
ICRP	: International committee or radiation protection
SSNTDs	: Solid State Nuclear Track Detectors
D	: Radon Diffusion Coefficient
VB	: Bulk Etch Rate
Rad	: Unit of absorbed dose
WHO	: World Health Organization
NCRP	: National Council on Radiation Protection and Measurements
AED	: Annual effective doses in units (mSv/y)
F	: Equilibrium factor is equal to (0.4)
H	: Occupancy factor is equal to (0.8)
D	: The dose conversion factor is equal ($9.0\times10\text{-}6$ mSv /Bq.m^{-3} .h)
Th	: Thorium
U	: Uranium
Rn	: Radon

PART 1

INTRODUCTION

1.1. NATURAL RADIATION

Since the Earth formed more than 4.5 billion years ago, the material from which it formed contained many radioactive elements. At that time, all the isotopes' short half-life dissolved, and only those with a long life of (100 million years or more [1]. Remained of rock deformation by physical processes and complex chemistry, which included many atmospheric changes as well as the movement of water [2]. Soil is the upper part of the earth's crust. Therefore, the soil weather changes and human activities affect the rocks of the Earth's crust. Soil considered radioactive because it contains many minerals, and its natural radioactivity can vary [3]. With various types of soil, the soil contains long-lived radionuclides such as ^{40}K and uranium isotopes and their decay chains. Basic radionuclides spread throughout the Earth’s crust. Basic radionuclides, which include most materials, have small amounts of ^{235}U, ^{238}U, and ^{232}Th, and these materials constitute the main sources of radioactive materials in the environment [4]. Naturally, many properties also differ from one element to another [5]. Physical processes differ in terms of mass and freezing point, as well as nuclear properties, which are very different. Isotopes that decay and are measurable can enable scientists to use decay to find out elements or things whose age we cannot know. This is in the name of radioactive dating, and (^{14}C) is the most famous technique for determining radiation dating. The Nuclear Regulatory Committee can define radioactive isotopes and materials as any substance capable of producing ions or specific radiation. A person exposed to radiation from natural sources, which includes cosmic radiation from terrestrial sources as well as radiation from radionuclides present in the human body, contains many radionuclides, such as (^{40}P), as well as the dissolution products of radon-222. More than 100 cosmic rays pass into the human body per second, and at the same time, the person inhales several radioactive atoms.

Of the CO_2 in the air inside the lungs, two or three uranium atoms reach his drink and food, and a few thousand potassium atoms, and not only that, as the soil and building materials release more than 50,000 gamma rays that enter the human body, and this is completely normal [6].

In the soil, unnatural sources of radioactivity are mainly artificial, such as using condensed fertilizers rich in phosphates used for agricultural purposes, as well as the discharge of permissible low-level liquid wastes and the Arab release into the environment from the Nuclear Fuel Cycle. with naturally occurring radioactive materials (NORM), in addition to air-explosions of nuclear devices. Previous and some accidents at nuclear plants, such as the Chornobyl plant, and these factors cause a strong increase in the exposure of residents to radiation [7].

Lately, there has been a growing fascination with naturally occurring radioactive materials, which are the primary contributors to the public's exposure to both natural and artificially enhanced sources of radiation.

The annual effective dose of exposure per person to natural radiation is 2.4 mSv, while all human sources are 0.8 mSv [8].

The United Nations Scientific Committee on the Effects of Radiation estimates that the nascent nuclides resulting from the curvature of radon gas are about three-quarters of the annual dose that humans receive from natural sources. [9]

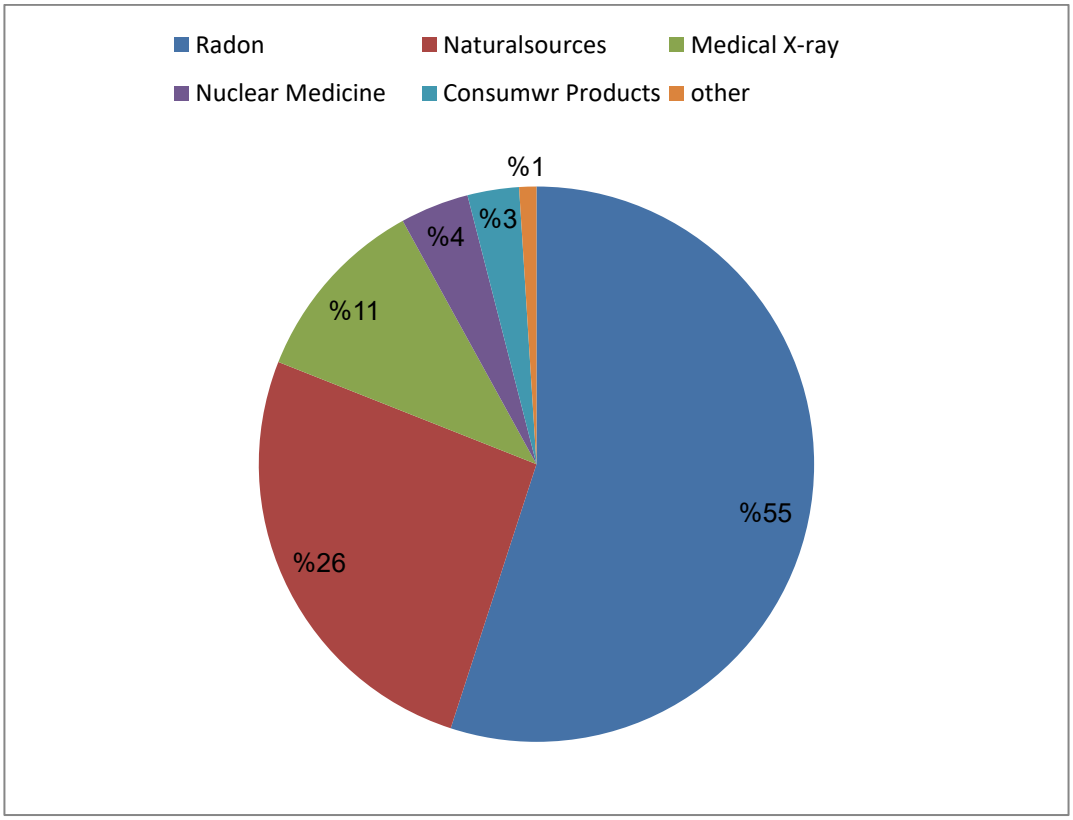

Figure 00.1. Annual dose from radioactive sources affecting the human body.

Multiple research have demonstrated the utilization of various methodologies for the estimation of radiation levels. We utilized CR-33 solid-state nuclear trace detectors to measure the levels of exposure in our present investigation.

1.2. TYPES OF RADIATION

Scientists can infer the types of radiation through many parameters such as charge, mass, etc., but there is a simpler way in which scientists distinguish the type of radiation, such as the amount of energy. Radiation with low energy called non-ionizing radiation, while radiation with high energy called specific radiation. [10].

1.2.1. Non-Ionizing Radiation

One variant of Electromagnetic radiation characterized by approximately 100 nanometers and a relatively low photon-energy, measuring less than 12.4 eV. Dieses energy level is inadequate to dislodge electrons from their orbits. However, it can adequately displace atoms within matter particles or induce their oscillation, as observed in radio waves, microwaves, and visible light. [11].

1.2.2. Ionizing Radiation

This form of radiation possesses enough energy to ionize, meaning it can remove an electron from an atom, resulting in the excitation of the atoms in the substance it interacts with [18].

Electromagnetic radiation possesses a brief wavelength [11] and has the capability to release a significant quantity of energy inside a confined area. Without a doubt, the acquired energy surpasses 33 (eV). Each ionization event has the capacity greatly disrupt the chemical bonds connecting two atoms.

Hence, all forms of ionizing radiation possess the capacity, either directly or indirectly, to dislodge electrons from most atoms. These radiations can be either particulate, alpha particles, or Electromagnetic, such as X-rays and gamma rays [12].

1.2.2.1. Alpha Particles

The nucleus of ionized helium atoms ($^{4}_{2}He$) consists of two protons and two neutrons. Alpha particles, released from naturally decaying radioactive elements, at speeds somewhat slower than the speed of light. They can penetrate the air up to (5 cm) before making them active ions with a short range of motion [13]. Therefore, they have a greater mass and exhibit a lower velocity compared to alpha particles, which are other forms of decay emissions. It can be stop easily. However, alpha particles have the ability to disrupt chemical bonds, potentially leading to chemical or biological harm,

by virtue of their dimensions, mass, and charge. The extent of its penetration into materials depends on the energy it produces and the materials it passes through thin materials like paper or skin can efficiently absorb alpha particles. Nevertheless, the ingestion or inhalation of alpha emitters might result in substantial damage.
. The main sources of alpha particle emissions are uranium (^{238} U), radium (^{226} Ra), and radon (^{222} Rn).

1.2.2.2. Beta Particles

During radioactive decay, certain unstable atoms release a beta particle. Beta particles can possess either a negative or positive charge, and they possess an extremely small mass (1/2000th the mass of a neutron), irrespective of the charge. The particles in question referred to as a negatively charged beta particle, an electron, and a charged beta particle. Positively charged particles known as positrons, beta particles have a greater ability to penetrate than alpha particles (the extent of their penetration influenced by the energy of the beta particles and the materials involved). Nevertheless, they can be effective halted by a thin layer of aluminum.

1.2.2.3. Electromagnetic radiation

Gamma ray, a form of Electromagnetic radiation, are associated with two categories of Electromagnetic waves. Gamma ray released when energy transitions from a higher-energy-state to a lower-energy-one.

Gamma rays often possess higher energy levels than Electromagnetic radiation released due to the transition of an atomic electron. It yields a certain amount of energy. The energy levels are denoted as x-rays. These rays can permeate matter to a greater extent than any other particle due to a portion of their energy that can only be halted by high-density substances like lead and concrete.

1.2.2.4. Neutrons

They are particles 2000 times larger than beta particles and have a mass 1/4 of alpha particles. Neutrons have a net electrical charge equal to zero and a higher ability to penetrate matter deeper than any other charged particle, but this naturally depends on the material and atomic nature of the penetrating material [13].

1.3. RADIATION SOURCES

Radiation refers to the transfer of energy through space and includes Electromagnetic waves, quanta (photons), and atomic particles such as electrons, neutrons, and protons [14].

Atom nuclei can be classify into two types: stable nuclides, which do not undergo spontaneous transformation into other nuclides, and unstable nuclides, which show evidence of spontaneous transformation into other nuclides. Radioactivity is the process by which an unstable nucleus undergoes a phase transition to become a stable nucleus, resulting in the emission of negative and positive alpha (α) particles, beta (β) particles, and gamma (γ) rays, which are positive and negative Electromagnetic waves, to transform into more stable nuclei [15].

Exposure to such radiation can be either from natural sources or from human participation in spreading radioactive materials, whether directly or indirectly [16].

Activity sources classified or separated into different groups. Humans exposed to radiation from two main sources

1.3.1. Natural Radioactivity

The sources of natural radiation exposure include cosmic rays originating from outer space and radioactive substances present in the Earth's surroundings, including the human body. Approximately 85% of the global population's average annual (l 2.4 mSv)

exposure dose is attributed to the dispersion of natural radiation sources, as reported by UNSCER in 2008.

At sea level, interactions with cosmic rays account for 15% of the total dose from natural sources. Latitude and altitude are key elements contributing to variations in the dose rate caused by natural environmental exposure. Specifically, the dose of cosmic rays at higher altitudes thought to be larger. The inhalation or entrance of radionuclides is significantly higher at higher altitudes than at sea level.

Ingesting primitive radionuclides via food can result in internal organ irradiation. Radioactive elements, such as Radon 222Rn, which is formed when Uranium 238U breaks down, can enter the human body through breathing and result in internal radiation exposure. In addition to cosmic radiation, other forms of radiation also occur.

Terrestrial in nature it originates from naturally existing primitive radionuclides that are present in the Earth's crust. Most of these nuclides belong to the uranium ^{238}U, thorium ^{232}Th, and uranium ^{235}U series [17]. In addition to these series, there are anther naturally occurring radioactive elements such as ^{40}P, ^{40}K, ^{87}Rb and others that release radiation.

The distinguishing characteristics of radioactive isotopes in decay chains are their varying half-lives and atomic numbers equal to or greater than the atomic number of lead, which marks the end of all chains. Nature consists of three radioactive series: uranium, thorium, and actinium. The neptunium series, which terminated in nature, brought to an end by the limited lifespan of its isotopes. These series mostly release alpha particles, beta particles and gamma rays [18].

1.3.2. Artificial Radioactivity

Another source of radioactivity stems from human activities, specifically the exploitation of radiation. These activities can result in elevated exposure to radiation from natural sources. Examples of such activities include the release of radioactive materials into the environment from nuclear power plants and the worldwide

dispersion of radionuclides through the deployment of nuclear weapons. The atmospheric recession caused by radioactive gases, such as the Chernobyl reactor accident Nevertheless, serves as the primary contributor to the yearly radiation dosage that the population subjected to [19]]. Radiation globally used for medical applications. Radioactive isotopes are collected within nuclear reactors by bombarding stable isotopes with different nuclear particles, including gamma radiation, protons, fast neutrons, and alpha particles. These particles either produce by accelerators as highly charged particles or serve as neutron sources. They also act as a source of fast neutrons, or gamma rays. The user states that scientists have successfully produced approximately 300 radioactive ions [20].

1.4. BIOACTIVE EFFECT OF RADIATION

Radiation exposure can occur through either internal or external means. Internal exposure arises when individuals ingest or consume water that has been contaminate or when they inhale air that has been taint with radiation. Radioactive particles can penetrate the body through skin wounds. Alpha and beta radiation are sources of internal exposure, while exterior exposure can be cause by beta radiation. Gamma and X-rays can permeate objects. Exposure to both exogenous and endogenous radiation can result in direct cellular harm [20]

is enclosed in square brackets. Exposure to substantial doses, particularly those associated with significant incidents such as nuclear weapons blasts, can have severe consequences, including fatalities arising from excessive radiation exposure in accidents. Workplaces are often the setting for fatal events. In addition, individuals who are exposed to high lethal doses may experience symptoms including skin burns, skin cancer, hair loss, and temporary or permanent infertility in males. In females, depending on the dose, infertility is typically permanent but requires a higher dose. Exposure to Rad 400 (and at Rad 200) can also lead to cataracts, which is the clouding of the eye lens [21]

Nevertheless, when individuals exposed to effective levels, they will change their genetic characteristics. Exposure to it can lead to chromosomal harm in the

reproductive cells of the individual, which might manifest as genetic abnormalities, birth deformities, or other ailments in subsequent generations. The consequences arising from exposure during pregnancy, specifically one of the subsequent physical impacts, suggest the occurrence of deformity. The genetic effect arises from the direct exposure of the radiation rather than the exposure of the parent's reproductive cells. The observed effects of prenatal exposure will vary depending on the specific stage of development at the time of exposure [22].

PART 2

PREVIOUS STUDIES

Knowing and understanding prior research, as well as anything associated with the topic of the study, is an essential first step. Confident in the proper course of scientific inquiry, eager to learn from and gain from the achievements of others in the field of inquiry, their discoveries, and the obstacles they have encountered. There has been unreported research undertaken. There have been several studies on using Solid State Nuclear Track Detectors (SSNTDs) to measure radon concentrations in buildings.

2.1. SOME TURKISH AND INTERNATIONAL STUDIES USING THE CR-39 DETECTOR

- In 2004, the Turkish researcher Köksal and colleagues tested the radon levels in buildings.
- The nuclear track detector CR-39 was used to measure the average indoor radon concentration in Turkey, which was found to be (105±52Bq\ m3) on an annual basis, 65Bq.m-3 in the summer, and 149Bq.m-3 in the winter.[23]
- The nuclear track detector CR-39 was used by the Egyptian researcher (Sroor, A) and others in the year (2001) to measure radon concentrations in southern Egypt. The findings indicated that the levels of radon concentration varied between 1.54 Bq/m3 and 5.37 Bq/m3, and found to be within the acceptable thresholds for these particular samples [24].
- The researcher Karpiska compared the indoor radon concentration in housing and soil in two regions of the geological places of Poland in 2002, and the researcher discovered that the average concentration in moving air is 301 Bq/m3 in the basement. Out of the 54 measurements of radon concentration in rocky areas, the study discovered that in eight instances, the concentration exceeded 200 Bq/m3. Additionally, in three cases, the results were greater than

400 Bq/m3. The highest percentage of radon found in homes with dirt basement floors and an entrance, and the study found that radon concentrations in these homes ranged from 587 Bq / m. directly to kitchens and rooms.[25]

- In 202 homes, the Chinese researcher (Tokonami) examined the radon and thoron concentrations in 2004. Over six months, indoor radon levels found to range between 19 and 195 Bq/m3.[26]
- Sainz compared radon exposure data for several Romanian areas in 2009. The greatest levels found close to the former uranium mines and between the areas of Spain where measurements taken using the CR-39 radioactive trace detector in 91 homes in Spain and 280 A homes in Romania. Values in Romania are 2650 Bq/m3 and 366 Bq/m3, in Spain respectively [27].
- Solid-state nuclear trace detectors (SSNTDs) type CR-39 were used by (Németh) and others in 2010 to monitor the levels of radon and thoron in households in Hungary that were close to a mine, the results indicated that residences generally had a radon level of 152 Bq/m3 [28].
- Obed et al. conducted a radon study in southwest Nigeria in 2011 using the CR-39 nuclear trace detector in 35 secondary schools where the detectors had been install for three months. For the locations examined, the average radon concentration was 45 ±27 Bq/m-3.[29]
- Using the CR-39 nuclear trace detector for two months, (Madureira) conducted a study in 2016 to measure indoor radon concentrations for public primary schools in Portugal analyze the key factors influencing radon levels inside buildings, and estimate the effective doses for students and teachers. The proportion of radon in all of the schools ranged from 56 Bq/m3 to 889 Bq/m3 for the yearly effective dosage, at a rate of 197 Bq/m3 and ranging from (0.58mSv to 3.07mSv) [30].
- Utilizing CR-39 detectors, Silva and Dinis, the two researchers, conducted measurements of radon levels throughout Portugal over the entirety of the 2017 calendar year.
- The reagents made available for a while (on average 42 days). Cases the radon concentration was higher than the suggested reference level (300 Bq/m3) and the protective threshold (400 Bq/m3) set out by Portuguese law. The necessity to increase worker radiation protection from ionizing radiation shown by

annual effective doses obtained from outside radiation and indoor radon concentration.[31]

- Al-Khateeb in (2012) evaluated radon concentrations in soil and closed areas for seven communities in the Ajloun region of Jordan. The findings revealed that the typical radon concentration steadily declines as the floor level rises, with the bottom floor having the maximum concentration (35.5±5.0 Bq/m-3) and the second floor having the lowest concentration (22.9±3.2 Bq/m-3). The living rooms had the lowest concentration, which was 33.8±34.4 Bq/m-3, while the storage rooms had the greatest concentration (8.8±5.4 Bq/m-3). In these villages, the average radon concentration in enclosed spaces was 36.3 ±2.3 Bq/m-3, and the effective dose- performance over a year was 0.92± 0.06 mSv.yr-1. These ratios fall below the International Commission on Radiation Protection's recommended work limit.

PART 3

THE THEORETICAL PART

3.1. INTRODUCTION

The primary purpose of most ionizing radiation measurements is to create a quantifiable relationship between these data and the biological, physical, and chemical impacts of radiation. A radiation measurement device consists of two main components: the detector, which detects radiation, and the radiation measurement equipment, which used to measure the radiation.

When radiation strikes a detector, one of two things happens: either the radiation produces a signal in the detector or causes a change in its characteristics. The detecting devices used for a variety of purposes, such as counting the number of nuclear particles that fall on the detector over time, identifying the kind and energy of the falling particles, calculating the radiation doses for radiation workers, and preventing exposure [32]. Since ionization is a crucial process for radioactivity, all detection techniques rely on the interaction of radiation with matter. Most detectors pick up signals caused by falling ions and electrons, which allows us to distinguish between radiation and other types of detectors. Active detector and passive detector are the two categories.

3.2. ACTIVE DETECTORS

The most crucial distinction between active and passive detectors is the great sensitivity to alpha particles. They need electrical energy for their work. The categories of active detectors are:

3.2.1. Gas Detectors

The collection of electric charges that arise from the ionization of gas atoms or molecules when ionizing radiation passes through it is the principle of the operation of gas detectors. Some of the earliest detectors are gas-filled devices that can detect radiation, and they sometimes referred to as counters.

[33]. Along the course of the fast-moving particle's motion within the gas, a reaction will take place to generate ionic molecules and excited molecules; as a result, an ionic pair that serves as the foundation of electrical impulses created. Regardless of the precise mechanisms, the number of ion pairs formed along the radiation path, is important to us [34].

Ion pairs can be form by direct interaction with the particle or through a secondary process in which some of the particle's energy transferred to an active electron or variable rays (Delta ray). Some gas detectors are ionization chambers, proportional counters, and the Geiger-Miller counter.

3.2.2. Scintillated Detectors

Ionizing radiation can induce the excitation of different materials, resulting in their rapid emission of light and the production of luster or brief bursts of light within microseconds of the stimulation. When particles collide with phosphorescent material, flash counters produced. The quantity of light produced is related to the energy and may be used to calculate the energy of the particles. Thermo-luminescent and sodium iodide detectors are two examples of scintillation detectors. The sodium iodide detector is one of the most popular detectors when directly measuring since it employs

sodium iodide triggered with crystalline thallium. Scintillator detectors may be use to detect neutrons because a crystal comprising zinc sulfide and paraffin is employed because it has a significant amount of hydrogen. This crystal used as a scintillator to detect gamma, which is used to measure ionizing radiation in a given location and at a certain instant. When a flash of light of the zinc sulfide released, it captured in the multiplier tube [32]

3.3. PASSIVE DETECTORS (SSNTDS)

This technology has arisen with several applications in diverse domains, including nuclear and space physics, cosmic rays, meteorite and lunar investigations, reactors, particle accelerators, and its utilization in mining. The production of these detectors took place in the late 1950s of the 20th century.and during the subsequent decades, they developed a lot until they became widely used in various scientific fields. In our current study, the nuclear trace detector (CR-39) used due to its high detection efficiency and good sensitivity to low particle concentrations in biological sciences, earth sciences, medicine [35], and environmental research, including its use in detecting alpha particles. In 1958, the scientist Young, employed at the Atomic Energy Research Corporation in Harwell, England, noticed the emergence of patterns in lithium fluoride (LiF) crystals that treated with a combination of acetic acid (CH3COOH) and hydrofluoric acid (HF). The number of tracks is directly proportional to the quantity of uranium fission pieces. [36]. The two scientists (Barnes Silk) observed linear damage in the thin mica sheets irradiated with fission particles in 1959 while they are working for the Atomic Energy Research Corporation in Britain [36]. As they created a new kind of track detector at the start of the seventh decade of the previous century, a team of scientists from the General Company for Electronics and the Research Development Centre in New York refined the new (SSNTDs). The light microscope seems to be able to detect fission fragment tracks in the microphone after the etching procedure [37]. Therefore, solid insulating or semiconducting materials that can maintain the influence of radiation resident at normal pressure and temperature circumstances may be refer to as nuclear track detectors [38]. Dielectric track detectors (DTE) commonly called such because they compose of dielectric materials and rely on abrasive solutions to uncover the areas of damage caused by ionizing radiation.

3.4. TYPES OF TRACK DETECTORS

Solid-state nuclear detectors have been employ to accurately measurement of radiation energy based on ionization. These detectors exhibit distinctions from ionization chambers, Geiger-Mueller counters, and proportional counters. These detectors have been use for a long time for radon measurement because they are very sensitive to alpha particle emitted from radon [39]. According to Figure (2.1), it comes in three types: crystalline, vitreous, and plastic [40].

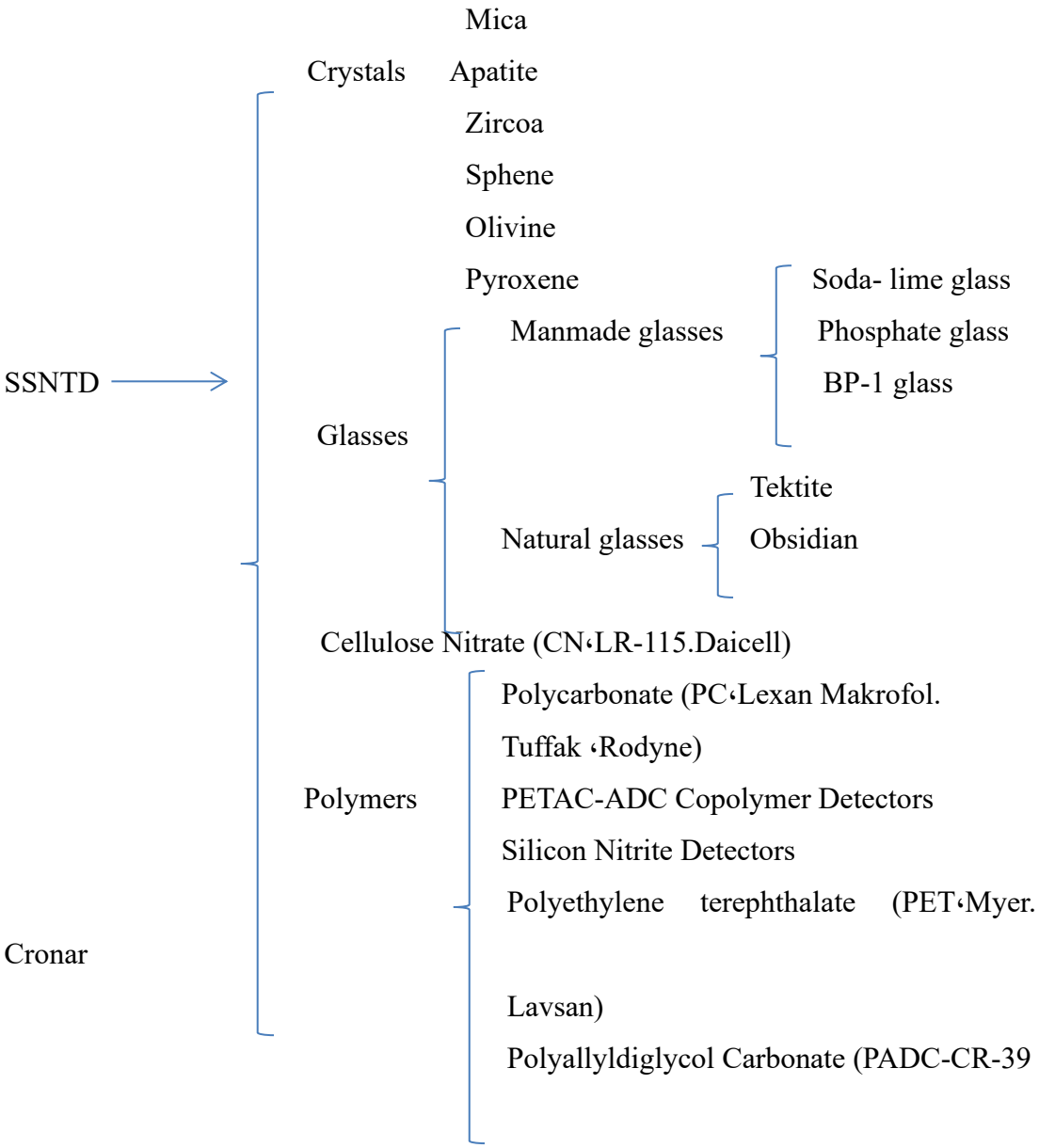

Figure 0.1. Diagram of kinds of track detectors [40].

3.4.1. Crystalline Solid Detectors

Ionizing radiation may be detected using solid, transparent materials like manufactured and natural crystals. The earth's crust, soil, rocks made of minerals, and dust are all rich sources of crystal materials. They regarded as natural suppliers of crystals. There is a distinct crystal structure for each kind of solid crystal. It is not composition contains both carbon and hydrogen, and each crystal has a variable abrasion rate in each direction [41]

Zircon, Apatite, Mica, Pyroxene, and Olivine are examples of the several categories of solid crystal reagents.

3.4.2. Crystalline Solid Detectors

Because it contains no carbon, glass categorized as an inorganic detector. High homogeneity and consistency of their qualities are their most significant traits. It is very transparent to light. It is a reliable detector for gauging reactor neutron flux and spotting fission fragments. The ages of geological samples (DTF) [42], may likewise be ascertain using this method. Due to its 40% effectiveness compared to cellulose nitrate detectors' 100% efficiency, glass considered less effective than mica and organic plastics in detecting fission fragments. Additionally, since glass tracks have limited lengths, a certain range of wavelengths must be use to identify fission fragments. The mass and energy of the fission fragments may be classify into industrial glass detectors and natural glass detectors [41] and do not all exhibit etched evidence [43]

3.4.3. Polymers Solid Detectors

Plastic detectors, which are polymers of organic detectors, categorized as huge molecules made up of several smaller molecules known as monomers connected. Occasionally, a covalent link established between the monomer units, where the hydrogen-carbon H-C bond assumes a prominent role. Organic polymers are notable for their composition of halogens, Sulphur, carbon, hydrogen, nitrogen, and oxygen

atoms, along with other elements. What distinguishes them is that the majority of the bonds between these atoms are weak and susceptible to breaking when exposed to ionizing radiation. [44].

The most popular solution is sodium hydroxide solution, which is prepared with a standard of (6-7 N) and at a temperature of (70^{o}C), and the most popular type of polymeric detector is the nuclear track detector CR-39 used in our current study. In general, the solutions used in detecting tracks with polymeric detectors are often solutions of alkaline hydroxides such as (KOH) and (NaOH) with a standard of (1-12 N) and a temperature of 40^{o}C to 60^{o}C. [45]

3.5. POLYMER TRACK DETECTOR (CR-39)

The CR-39 detector is one of the best solid plastic organic detectors. CR-39 is another name that used experimentally. It first discovered in 1978 by Cartwright and Shirk. its molecular formula $C_{12}H_{18}O_{7,}$ and its density 1.32g/cm^3 [46]. The substance is Poly allyl diglycol carbonate (PADC), which possesses a lattice structure that cross-linked. It is crystalline, with a crystallinity level of up to 20%. The material's monomer contains carbon bonds, which are rather weak and susceptible to breakage when expose to radiation or ionizing particles, and it does not contain nitrogen in its composition. The proportions of oxygen, carbon, and hydrogen in its composition are (6.56%, 52.554%, and 40.87%), and its corresponding molecular weight is 274 [47]. The monomeric structure of the (PADC) detectors consists of two groups of alleles (-CH - CH = CH). as shown in Figure (2.2).

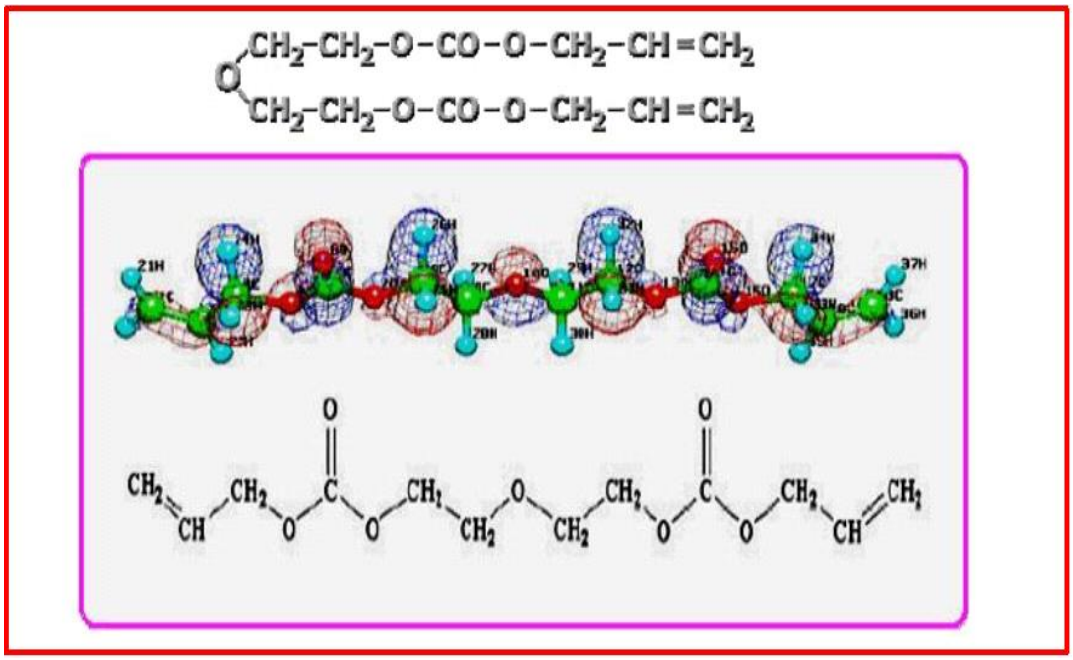

Figure 0.2. Chemical composition of the CR-39 track detector [48].

Two researchers, Shirk and Cartwright, identified the fundamental characteristics of the CR-39 detector, which include uniformity of its structure, regularity, optical transparency, and high radiation sensitivity, such that the change in its reaction does not exceed 1%. A more homogenous polymer termed CR-39 Dope produced by adding Phthalate Dicot Dope to the detector's monomer before polymerization [49]. The SR-86 detector created and made more sensitive by several tests, while the detector CR-39 developed and refined. The BM-355 detector, BM-500 detector, and BM-600 detector, all built of the same CR-39 material, are some of the other varieties that have been create from this detector. Because the tracks of protons and neutrons are clear and have enormous diameters, this detector, also sometimes referred to as New Super Grad CR-39, has been manufactured to be more suited for these tracks. Because of its benefits and positive traits in medicine and biological applications like measuring radioactive nuclei doses in the airways, lungs, and blood that produced a result of inhaling air contaminated with radon. In measuring uranium present in dental materials, the CR-39 detector is among the most widely used types in many applied fields and fields of science for a wider range of energies. It distinguishes itself through its exceptional sensitivity to charged particles and various energy levels, as well as its ability to detect and record the paths of protons across a wide range of energies. It is notable for its exceptional thermal stability, optical purity, high transparency,

uniformity of constituent materials, similarity of their properties, resilience to moisture, pressure, and heat under standard storage conditions, and outstanding resistance to high temperatures. Using conventional chemical etching, the detector is capable of detecting charged particles with energies as low as 200 keV, which serves as the minimum threshold for detection. The utilization of a chemical process employed to illustrate the impact of charged particles in nuclear track detectors. Additionally, physical and chemical factors of the detector and the etchant solution, such as the concentration of the solution and the density of the detector, as well as electrical and mechanical etching rates. These parameters affected by the density of the ion's accumulated lost energy along its path in the detector as well as the type of chemical solution used in the etching, as well as the storage conditions of the detectors [50].

3.6. CHARACTERISTICS AND APPLICATIONS OF POLYMERIC TRACE DETECTORS

Due to its benefits and traits, nuclear track detectors used in a variety of applications, the most crucial of which are [45]

- It is useful for activities where it is challenging to employ electrical instruments, such as the core of a nuclear reactor, space exploration, and detection of low amounts of radiation over extended for a period time, thus it does not need an electric power supply.
- It is inexpensive, simple to use, and reasonably simple to etching effects.
- Mica and plastic detectors, it characterized by high efficiency and sensitivity that may exceed 90%. In order to measure neutron dosages or neutron flux, it counts the tracks left behind by protons hitting neutrons or by alpha particles produced during the (n, α) reaction.
- Its capacity to maintain the shape of the radiation effect (damage) under normal temperature and pressure circumstances, since high temperatures cause the effect to partly or totally heal, which lowers the number of effects that are created in it.
- Precision in measuring a variety of dosages.

- Due to its great homogeneity and symmetry, it does not dissolve in chemical solutions and cannot be dissolve by chemical etching solutions, although it may decompose and lower its thickness.
- These detectors used to assess the radiation doses to which the population exposed since they provide accurate findings and are simple to analyze.

3.7. THE RADON (RN)

Radon (^{222}Rn), is a noble gas with a relatively long-life and simple mobility to travel large distances under various geological circumstances, it is one of the principal components in the natural radioactivity of the earth's crust. In geological settings, radon's prevalence and transmission from the parent nucleus (^{226}Ra) are what determine it spread the most. All three radioactive decay series include radon isotopes: ^{219}Rn in uranium series ^{235}U, ^{220}Rn in thorium series ^{232}Th, and ^{222}Rn in uranium series ^{238}U. These isotopes' half-lives are (3.96s, 55.6s, and 3.824d) respectively. It was first knew as radium emission until 1923 when it started to be knew as radon [51]. Radon is a naturally occurring radioactive gas that discovered in the twentieth century (1900) by Dorn. Radon has mass number of 222 and an atomic number of 86. A stale, flavorless, and colorless gas known as radon is soluble in water and a radioactive element, meaning it may break down and generate other elements, everywhere in the crust of the planet, particularly in rocky and mountainous locations, it is present [52]. Since groundwater comes into touch with underground rocks that contain natural uranium on a regular basis and continuously emit radon gas, groundwater has far greater radon concentrations than water. Surface radon enters buildings as a gas via cracks and holes in the foundation or by dissolving in water. Surface radon originates in rocks and soil and travels from there through voids and fractures. Studies typically quantify the quantity of radon in air or water in units (Pico Curies) per liter of the respective medium. Since radon dissolves in water, particularly groundwater, it escapes from it when retrieved, especially if it is agitated, and as a result, the concentration of radon is extremely low in rivers and lakes [53]. We will measure the concentration of radon in units of Bq/m^3 per cubic meter throughout our investigation. Radon formerly thought to be beneficial and is present in certain natural spring waters. Due to that radon decay into a stable isotope of lead when it interacts with water, it

only produces solid breakdown products that will stay in the water [54]. A background of low-level natural radiation is continually present in the population. Natural radiation is often responsible for the maximum human dosage. Terrestrial, internal, cosmic radiation and radon are the four major components of primary natural sources, but exposure to medical radiation sources mostly caused by human activity [55].

3.7.1. Radon and Its Decay Products

It is a noble radioactive gas called radon, has long half-life (3.82 days). This gas inter human body by inhalation, which decay with alpha exception of a little quantity that transported by blood. Due to the radon's disintegration produces toxic byproducts, it is dangerous. The substance congeals in the airways and on the inner lung surfaces. The polonium isotope (^{218}po), having a half-life of (3.05 m), is followed by the lead isotope (^{214}Pb) with a half-life of (26.8 m), and finally the bismuth isotope (^{214}Bi) with a half-life of (19.7m), down to polonium (^{218}Po) with a half-life of ($t_{1\backslash 2}$=1.6x10^{-4}s). Two of them (^{218}Po, ^{214}Po) emit alpha particles with an energy of (6 and 7.69 MeV) respectively, which represent the mean source of lung damaging radiation [56]. The diagram of radon and thoron decay products shown in Figures (2.3) and (2.4).

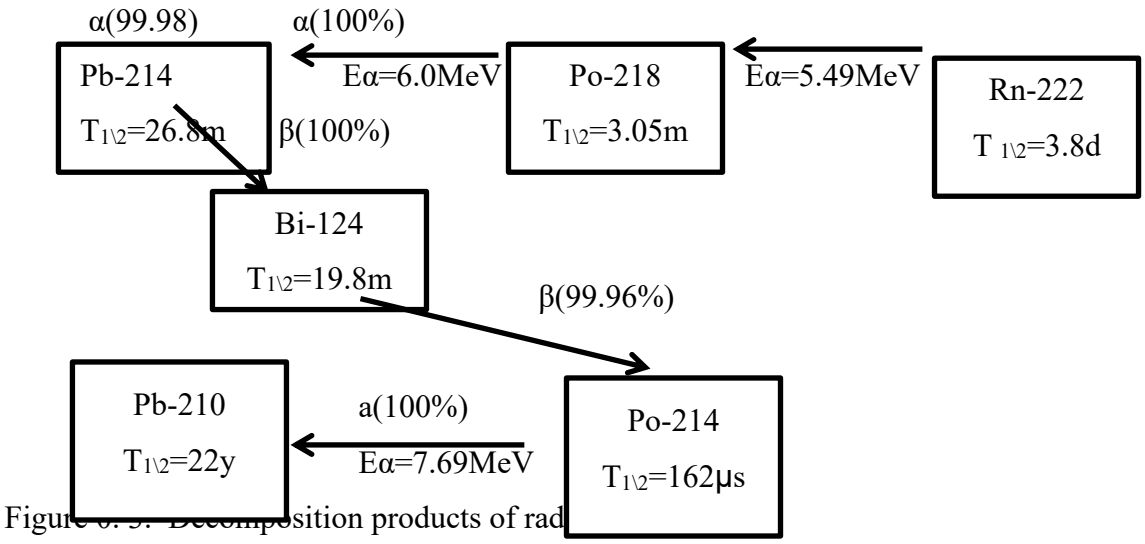

Figure 3.3. Decomposition products of rad

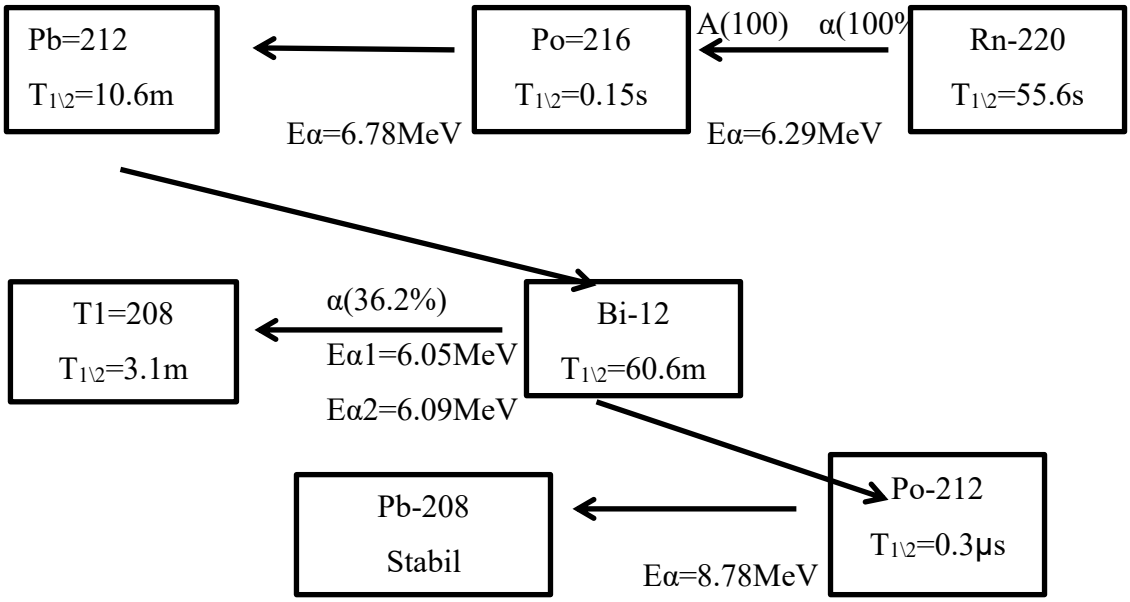

Figure 3.3. Thoron's decomposition [57].

3.7.2. Sources of Radon

All kinds of soil and rocks contain some radon, but the amount varies from area to region and season to season. When the gas released from the soil throughout different times of the year, it travels slowly in the open air and poses no health risks because of its half-life. However, what it introduces into enclosed areas, like buildings, depending on how concentrated in the soil and how the building was did, it might build up and reach hazardous levels. Radon may inter building via groundwater or radium-containing construction components.

3.7.2.1. Radon Sources in the Soil

At least 80% of the radon in the atmosphere produced by soil generated from uranium containing rocks, where ^{238}U decay into ^{226}Ra and radon gas. Because radon has a greater ability to move and spread than uranium and radium, it can leave sedimentary rocks that contain phosphates and metamorphic rocks derived from those rocks that have uranium rates higher [58]. Radon can also escape from these rocks through pre-existing fractures and openings as well as through the pores between soil grains as shown in Figure (2.5). The permeability and wetness of the soil are only two of the variables that affect how much radon released from it. The migration of radon production to the outside environment shown in Figure (2.6). According to studies, around 10% of the radioactive gas produced in the soil's meter closest to the surface, and emitted in to the surrounding environment [59]. The atmospheric pressure and carbon dioxide content in the soil, where carbon dioxide functions as a carrier of radon gas in the soil and may increase its concentration in both the soil and the atmosphere, are additional variables that contribute to the release of radioactive gas [60].

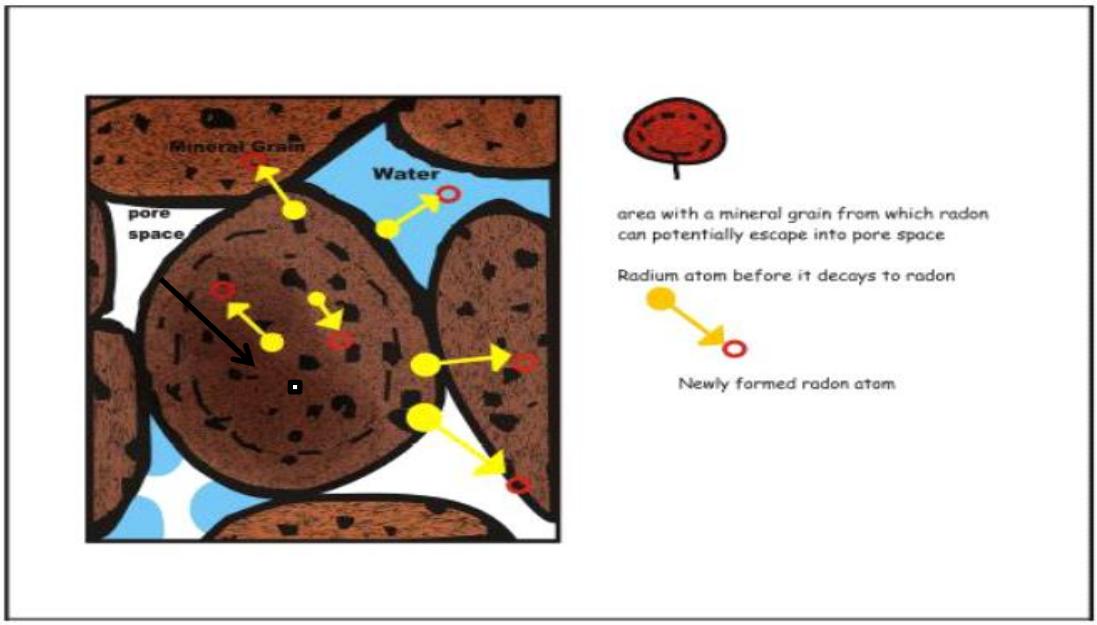

Figure 0.4. Radon spreads via the soil and rock pores [60].

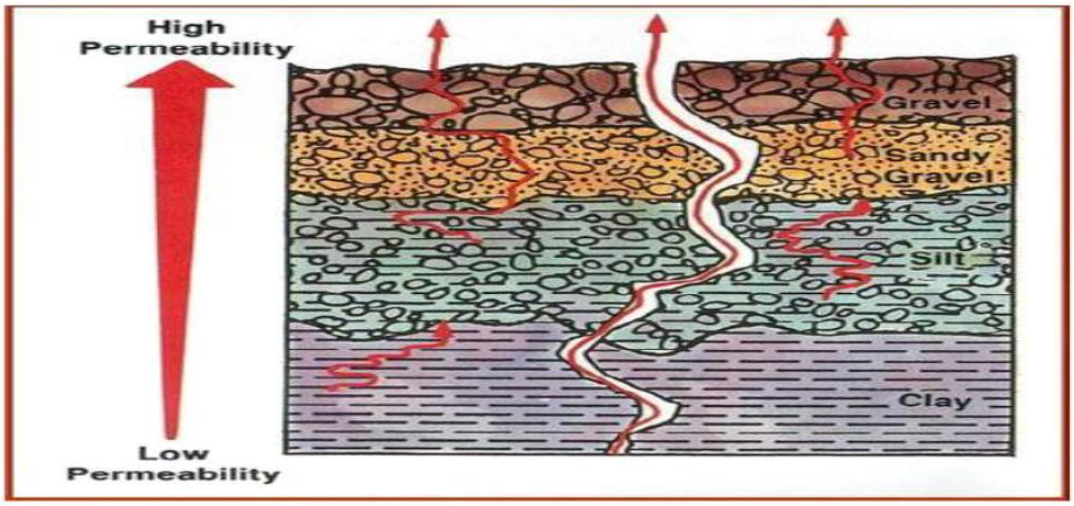

Figure 3.5. The flow of radon production to the external environment [59]

3.7.2.2. Water's Radon Sources

Water systems may let radon into a house. Because it escapes into the atmosphere, radon gas is often exceedingly rare in lakes, rivers, and reservoirs. Consequently, the issue of radon in water in major cities often does not affect residences that rely on surface water. Aeration of the water, which enables radon to escape while delaying the pumping and use of the water until the majority of the residual radon has dissipated, is the method used to treat water for big municipal systems. It transmits to residences in a hurry since it is closed. Because it prevents radon from being disposed of or from decomposing, it is spread throughout the population when people shower, wash their clothing, use the kitchen, etc. Groundwater is one usage that is likely to have radon issues, particularly in places with granitic rocks containing uranium. [61] Additionally, the rate of radon emission relies on the surface area of the water exposed to the air and is directly proportional to the increase in surface area. Both factors related to temperature. There is radon gas present, and some of it discharged into the environment when the temperature increases or is agitated [61].

3.7.2.3. Building's Radon Sources

The concentration of ambient air, ventilation rates, structural details, and central heating all affect indoor radon levels. Materials used in construction and societal customs [60] Radon gas enters residences from the ground via holes in hollow bricks,

fissures in concrete floors and walls, or spaces between walls and ceilings. It may also enter through and around water drainage pipes. Therefore, radon levels are often greater in basements, basements, and ground floors, as seen in Figure (2.7). The indoor radon concentration also changes from year to year, from day to day, and from hour to hour, depending on a variety of variables. Due to a lack of constant ventilation in buildings, particularly in nations with cold climates, it is greater than its concentration in the open air. Numerous studies have demonstrated that the kind of rocks and soil, as well as many other aspects of a home, such as the style of the house, the type of floor, the year of construction, the materials used, and the type of foundation, all affect the concentration of radon ^{222}Rn [62].

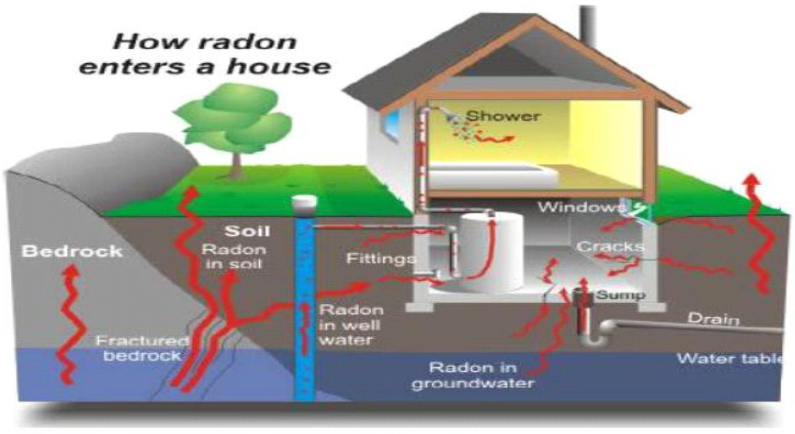

Figure 0.6. Sources of radon gas entering dwelling [63].

3.7.2.4. Radon sources in construction materials

Natural radioactive elements like uranium and radium are present in soil-derived building materials like cement, bricks, ceramics, etc., and as a result, they decay to produce radon, and that radon emitted into the atmosphere using these materials. Concrete, gypsum phosphate, flint, and fluorescent stones are a few of the materials that are more radioactive.

More than 40% of the radioactivity discovered within the structures since their floors, walls, and ceilings constructed of cement, sand, earth, and rocks, which have lower radioactivity than wood and natural gypsum materials. The concentration of radon in

buildings influenced by a number of different variables, including temperature and humidity [64]

3.7.3. Physical Characteristics of Radon

Radon cannot detected by human senses, because of it is a colorless, tasteless, odorless, non-flammable gas that emits alpha particles. It has a melting point of (-70ºC) and a boiling temperature of (60.8°C) It is seven times heavier than air and has a high gas density of (9.96kg\m^3). It may readily flow between the ground and the air since it is a noble gas [65]. Since it is the only noble radioactive gas, radon is a special element. At ordinary temperatures and pressure, it is chemically inert and one of the heaviest gases. In certain cases, radon gas is colorless. It includes brilliant phosphorous that, when chilled to the freezing point, becomes yellow with a drop in temperature and turns red-orange at the temperature of liquid air. The radon gas's physical characteristics are shown in Table (2.1) [66]

Table 3.1. Physical properties of radon. [66]

Name , Symbol , Number	**radon , Rn , 86**
Chemical series	Noble gases
The set, the period, the group	18،6،p
exterior	Colorless
Atomic mass	(222) g. mol^{-1}
Electronic distribution	[Xe] 4f ^{14} 5d ^{10} 6s ^{2} 6p ^{6}
Shell electrons	2,8,18,32,18,8
the condition	Gas
Melting point	202°k(-71°C)
boiling point	211.3◦k(-61.7°C)
Latent heat of fusion	3.247kJ.mol^{-1}
Latent heat of vaporization	18.10kJ.mol^{-1}
Heat capacity	(25°C) 20.768J\(mol. ◦k)

3.8. RADON'S HARMFUL IMPACT ON HEALTH

As we noted earlier, internal-radon gas exposure makes up a large portion of the radiation dosage that the population receives in many nations. Isotopes ^{214}Po and ^{218}Po are among the extremely tiny solid radioactive particles created by the disintegration of ^{222}Rn. These particles attach themselves to dust and natural airborne particles. These

specks will adhere to the bronchi after inhalation. As a result, alpha particles released which both raises and lowers the chance of developing lung cancer. The amount of radon, the length of exposure, and an individual's smoking behavior are the three main determinants of radon exposure [67]. Environmental research confirms that radon exposure raises the risk of lung cancer in the general population since the percentage of lung cancers linked to radon exposure to be the same. Depending on the calculating technique and the average radon concentration in the nation, the range is between 3% and 4%. In many nations, smoking is the leading cause of lung cancer, but radon is a close second. Smokers or those who have smoked in the past are at higher risk of getting lung cancer than non-smokers. There is currently no established safe level of radon exposure, despite the fact that it is the primary cause of lung cancer in non-smokers. Lung cancer risk may be somewhat elevated even in the presence of modest levels of radon. The connection between radon in interior environments has been the subject of much investigation since the 1980s. Likewise, research gathered data on lung cancer from China, Europe, and North America. The findings from all three of this research were gathered and analyzed centrally. When seen together, all three analyses painted a remarkably similar picture of the risk of lung cancer. After exclusion, they also proposed a rise in lung cancer risk to less than 200 Bq\m^3, which is the area for which the work published internationally [68].

3.9. PROTECTION AGAINST RADON GAS

The most crucial steps that must take to mitigate the radon in buildings. Future dwellings should have radon levels of roughly 100 Bq/m^3, according to the International Agency for Radiation Protection (ICRP) [69]since this will prevent radon from becoming the primary cause of sickness in the neighborhood. Ventilation techniques are among the greatest ways to decreased radon levels. The International Agency for Environmental Protection confirmed the activity of this method in 1986, and the operation of air conditioners in buildings and the purpose resulted in a decrease in radon concentration. The purpose is the fan that works to push or pull the soil gas away before it enters the house. Types of paint for securely seal the walls to decrease radon emissions. It also advised to utilize cement rather than concrete since cement has lower levels of radon gas than concrete with an air hole. Additionally, the presence

of radon in groundwater causes it to be absorbed from neighboring places, necessitating the use of water pumps from the nearby cities' pipelines. However, because the dissolved radon might be release, this approach requires the use of filters that absorb radon, which is costly. [70], [71]

3.10. MECHANISM OF TRACK FORMATION

The ionization process that these charged particles generated in the detector serves as the foundation for the notion of detecting the pathways that they take when they formed by the detector. The primary or secondary polymeric chains of nearby molecules and atoms are broken, or both simultaneously, as the ionizing body travels through the nuclear track detector material. Short polymeric chains with active ends and free radicals are produced a consequence through this process. Their numbers depend on how much energy the ion loses while traveling through the detector. Figure (2.8) describes how free radicals and chain formation occur in most polymeric nuclear detectors.

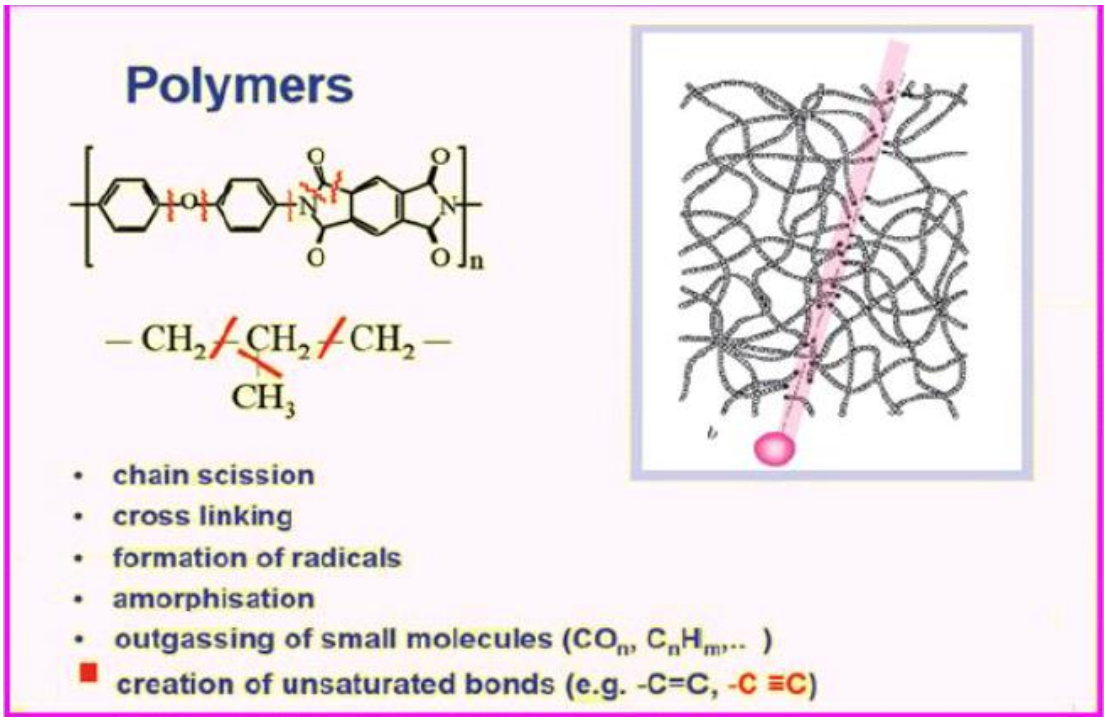

Figure 3.7. The primary and secondary chains in break along the passage of the charged particle.

This procedure results in the formation of a radioactively damaged cylindrical zone with a diameter of about 50,000 [72].

The repulsive force between the positive ions generated in the damaged area causes them to repel each other. Alternatively, we can etch this area with appropriate chemicals, then examine the etching tracks under a microscope (Fig. 2.9). The schematic diagram shows the stages of track formation in a plastic detector, including the oblique and perpendicular fall of particles on the detector, the track etchant rate (V_T) along the particle path toward depth in the detector, and the general etchant rate (V_B) for healthy areas on the detector surface[73].

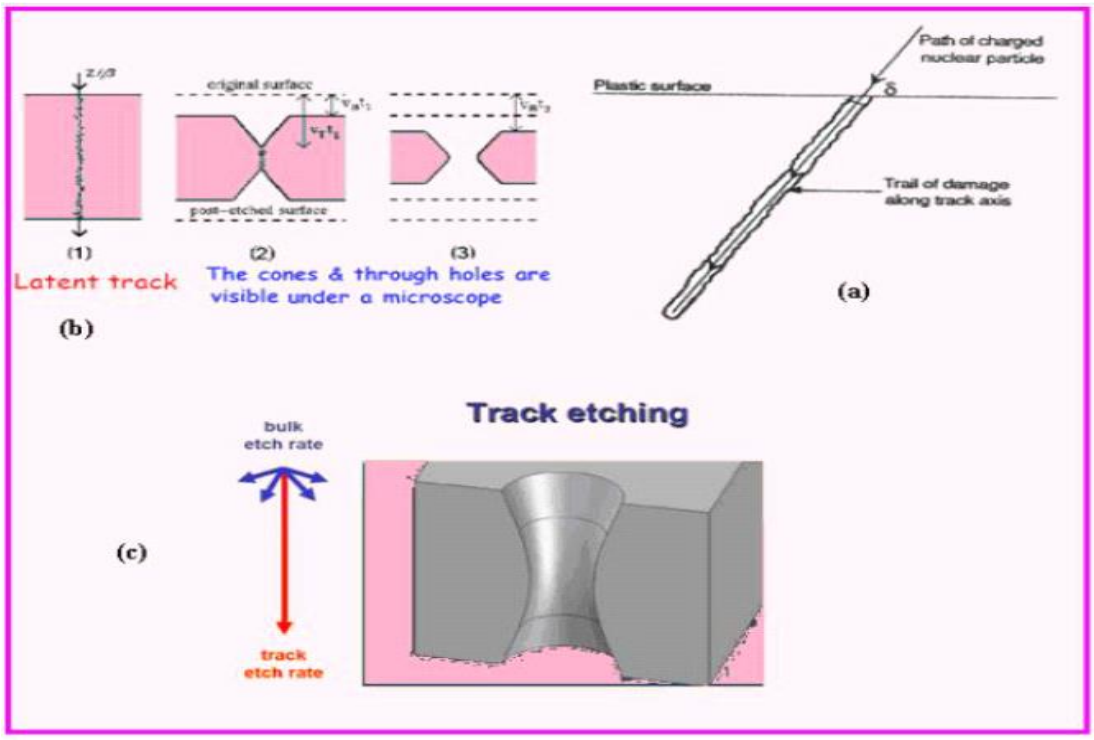

Figure 3.8. Tracks formation in the plastic detector.

(a) The oblique fall of the particle (b) the vertical fall (c) the impact scraping and the two modifiers of the scraping body [74]

According to the theory of the interaction of heavy charged particles with matter, when a charged particle passes through a material detector, it will lose energy through numerous collisions with the detector's atoms or by forming numerous ion pairs

(negative and positive). As the energy lost in each collision is very small and occurs along with the passage of the particle. After the first ionization step the material's charge produced by a number of different processes as following [75]

- Energy deposited in the first moments, followed by ionization, electronic excitement, and hot electrons, until the damaged zone starts to show after 10^{-17}-10^{-15} seconds.
- In a matter of 10^{-15}-10^{-14} seconds, the hot electrons started to cool, and the deposited energy began to spread, leading to the beginning of the electron aggregation process and the construction of the cold lattice.
- An electron-phonon connection occurs, called a Coulomb explosion, which starts the process of energy spreading to the atoms, heating up the atomic lattice, and eventually leading to fusion within 10^{-13}-10^{-12} seconds.
- Finally, a thermal spark with a sudden and quick cooling of randomly distributed atoms occurs at a time of 10^{-12} for metals and 10^{-10} for insulators, resulting in the appearance of defects or regions of damage, as shown in Figure (2.10).

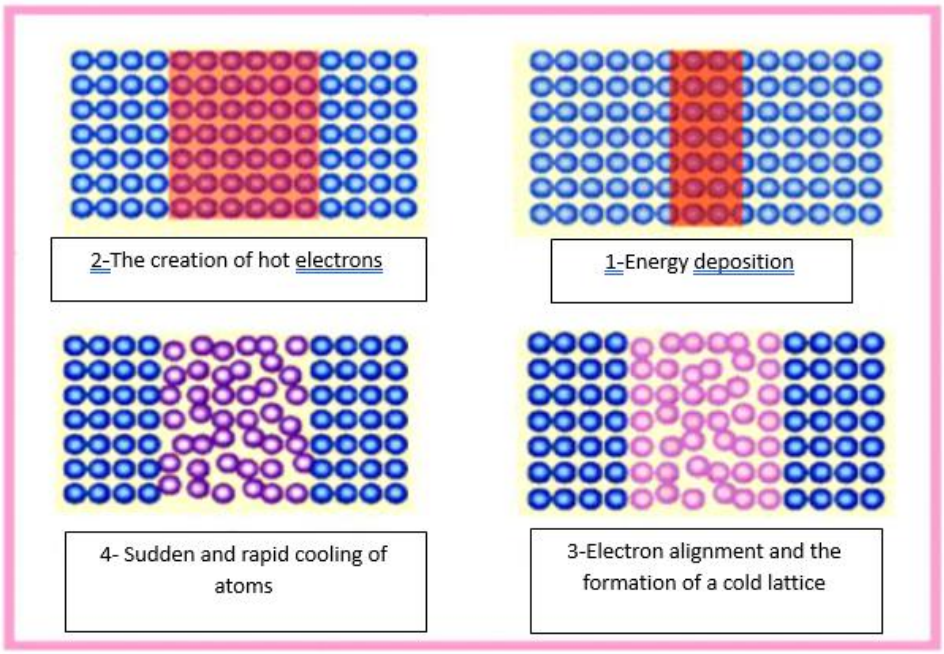

Figure 2.9. Steps in the creation of damage in the plastic detector [75].

Every dielectric solid has a threshold for the intensity of the effects. The threshold limit is the smallest amount of initial ionization that must be present to produce tracks capable of etching the ability to increase minimally the intensity of damage across the length of the core detected by etchant procedures is one of the key features of SSNTDs [76].

3.11. TRACKS APIARIAN

Tracks appear either directly using Electron Microscopy, Atomic Force Microscopy (AFM), and Confocal Microscopy to display the image of the 3D tracks, or indirectly by drilling or etching the damaged tracks and displaying them. There are several methods of etching techniques for tracks, including electrochemical etching (ECE), induced wave etching, ultrasonic chemical etching (UCE), plasma etching (dry etching) ,and chemical etching (CE).

3.12. CHEMICAL ETCHING

The most frequent kind of etching operation uses chemical solutions to assault the detector in general and more specifically target its damaged parts. This causes the detector's particles to dissolve at varying speeds depending on the location. When dealing with organic materials, the etching procedure carried out utilizing chemical solutions. An aqueous solution of potassium hydroxide (KOH) with a calibration of 6N and an aqueous solution of sodium hydroxide (NaOH) with a calibration of 6.25N used to carry out the procedure. In order to etched inorganic cross-linked materials like glass and mica, acid solutions—particularly hydrochloric acid with a concentration of 48% and a temperature of 23 °C [77]used. Etching done in a water bath that has a thermostat-controlled temperature range of 40 to 70^{o}C (and, in rare circumstances, up to 90^{o}C). The typical etching process takes somewhere between two and six hours. The volume increases with the strength of the etching solution, etching duration, and etching temperature. The outcome tracks in certain circumstances, (Ethyl alcohol) may be added to the etching solution at a predetermined rate, as in the case of (PEW solution), which is composed of A (ethyl alcohol and water) and B (potassium hydroxide). Alcohol helps certain plastic materials (polycarbonate) capture traces

more sensitively. The damaged areas were more brittle, and have a greater ability to dissolve and dissolve in the etchant solution because they have more potential energy due to the energy transferred to them from the particles. Their particles disintegrate more quickly than the particles of the healthy areas, even though it reduced by a decrease in some of them, such as CR 39 [78]. Conical tracks (pits), which can be seeing on the surface of the detector using an optical microscope, formed in the areas where charged particles fall into the detector when the rate of etching towards the depth of the track (V_T) along the damaged path is greater than the rate of general etching of the undamaged areas (V_B). Additionally, the widths of these tracks related to both the extent of the plastic detector's structural damage and the energy that the particles were able to transmit to it. Only particular circumstances allow for the process of excavating the damaged cylindrical routes beside the passage of the charged particle traveling through the detector, displaying the traces, and examining them under an optical microscope. When a charged particle effect the detector's surface at a certain angle of incidence. A conical hole must satisfy two requirements, one of which is the etching rate (V_T) along the damaged route towards the depth, and the second has to do with the particle's angle of fall on the detector (Θ). These two requirements must be met in order for the trace to emerge and for it to be seen under a standard optical microscope. The formation of an alpha particle after etching by a vertical and inclined fall is shown in Figure (2.13).[79]

The chemical etching process carried out according to parameters [80].

- Type and composition of etchant solutions.
- The concentrations of etchant solutions.
- The etchant solution depends on a suitable temperature.
- The time it takes for the etching process.

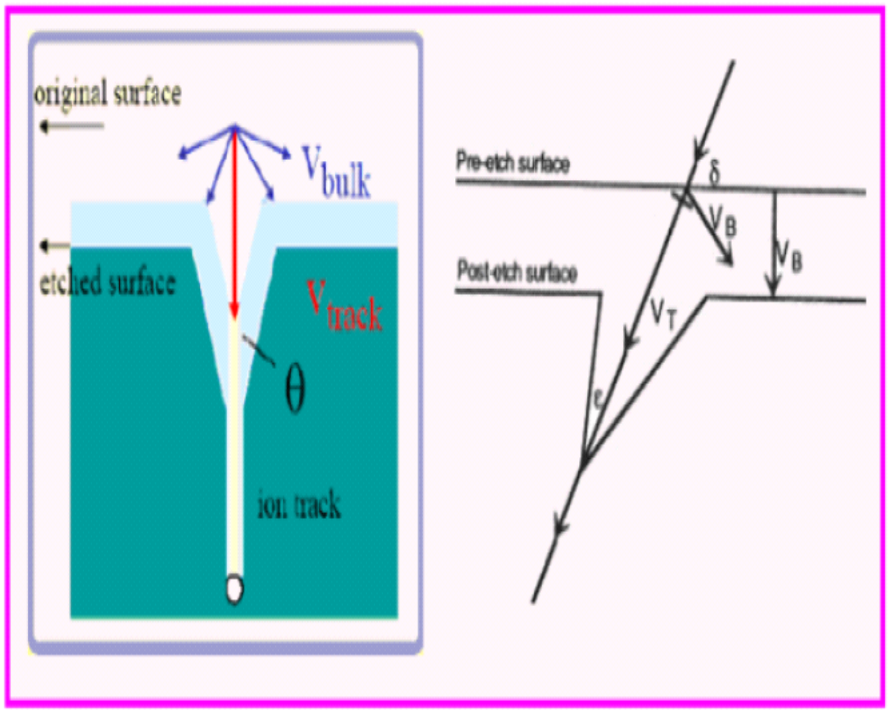

Figure 3.10. A particle falls on a detector perpendicularly and obliquely [124].

The angle of incidence (θ), meanwhile, is the angle made between the falling particle's path and the detector's horizontal surface. There is a need that must be satisfied, and that is the idea of the critical angle, in order to acquire the trace and the potential to examine it. The detector's critical angle (θ_c) is the angle at which detection is stopped. For a particle to be detected, this angle must be larger than or equal to the critical angle of the detector ($\theta^3\ \theta_c$), and it must also be at which the detection is stopped ($\theta = \theta_c$). represents the angle that determines whether the scraped trace will appear or not; if the charged particle strikes the detector's surface at an angle smaller than this angle, the etched track will not be visible to the detector. Whatever this angle may be, every detector has one [81]. Moreover, it varies from one detector to another. It relies on the detectors kind, origin, chemical makeup, etchant, and other environmental elements that may effect it, as well as the kind of particles used. In equation (2.1) the critical angle is stated.

$$\theta_c = \sin^{-1}\frac{1}{V} \tag{2.1}$$

V is the etching rate ratio were

Regarding the circumstance surrounding the etch rate (V_T) it well known that the majority of particles hitting the detector do so in an oblique fashion. Because the depth of the track formed by the etching rate (V_T) is less than the thickness of the layer removed, it is impossible to observe the tracks formed at the start of the etching process because (V_T Sin θ <V_B) the etched track formed completely removed by the etching process. Therefore, the prerequisite for the appearance of tracks must be the vertical component (V_T Sinθ ≥ V_B), assuming that the angle of the etching threshold and the etching process progress cause the (V_T) to grow in comparison to the (V_B), which is typically a constant amount until it reaches the value of one (V_T Sin θ \V_B=1). As the etching process continues, the rate of etching rises towards the depth and becomes (V_T Sin θ >V_B). It is important to note that the particle's vertical fall on the detector occurs at an angle of (θ = 90^o) and (sin θ= 1) [81]. In addition to the aforementioned, each detector is distinguished by having a crucial value for the charged particle energy loss rate known as the threshold energy (Eth). When charged particles lose energy over the threshold energy by themselves, they may leave behind trails or regions of damage that may be seen by the etching process [82].

PART 4

EXPERIMENTAL PART

4.1. DESCRIPTION OF THE STUDY AREA

Karabük Province is a landlocked province in the northern part of Anatolia (northern central Turkey), located about 200 km (124 mi) north of Ankara, 115 km (71 mi) away from Zonguldak, and 113 km (70 mi) away from Kastamonu in 2022 it had a population of 225,403. The main city is Karabuk located about 100 km (62 mi) south of the Black Sea. Because it is crucial to ascertain the levels of radioactive radon gas there, the research conducted in the Karabük Governorate. In the research, there were 15 new and 10 old homes. According to the rooms where people spend a lot of time as well as the rooms with little to no ventilation, different rooms from each home selected. Because building materials regarded as one of the most significant factors that affect the concentration of radon gas after the soil, both new and ancient structures selected for study.

4.2. MATERIALS

4.2.1. Nuclear Track Detector

The CR-39 nuclear track made in Britain by (Page Casting), with thick of 250 mm and has a surface area of about 1x1 cm^2. The first step in this work is to record the coordinates of the residential sites that chosen, and their symbols, which presented in table (1). Houses selected as follow, 10 old residential houses and 15 new houses in the summer season 2022, and 10 old and the same for new houses in the winter season 2022. One hundred eighty CR-39 track detectors distributed as follow, four detectors in each house, which suspended in the living and sleeping rooms for a period of one

month. These detectors were kept inside a sponge in suitable dimensions to preserve them as in figure 4.1.

Figure 0.1. The hanging of detector in a sponge

Table 4.1. The coordinates of the residential sites and their symbols.

Modern residential (new)					Old residential				
S. No.	North	East	symbol		S. No.	North	East	symbol	
			summer	winter				summer	winter
1	41°22' 07"	32° 66' 53"	S1na,b	W1na,b	1	41° 19' 81"	32°61' 68"	S1oa,b	W1oa,b
2	41°22' 23"	32° 66' 67"	S2na,b	W2na,b	2	41° 19' 82"	32°61' 67"	S2oa,b	W2oa,b
3	41°21' 95"	32° 67' 09"	S3na,b	W3na,b	3	41° 21' 17"	32°62' 49"	S3oa,b	W3oa,b
4	41°21' 18"	32° 62' 49"	S4na,b	W4na,b	4	41° 22' 01"	32°67' 30	S4oa,b	W4oa,b
5	41°22' 06"	32° 66' 54"	S5na,b	W5na,b	5	41° 22' 05"	32°66' 50"	S5oa,b	W5oa,b
6	41°21' 84"	32° 65' 44"	S6na,b	W6na,b	6	41° 21' 78"	32°65' 72"	S6oa,b	W6oa,b
7	41°22' 14"	32° 66' 06"	S7na,b	W7na,b	7	41° 13' 42"	32°39' 40"	S7oa,b	W7oa,b
8	41°22' 07"	32° 66' 00"	S8na,b	W8na,b	8	41° 13' 42"	32°40' 03"	S8oa,b	W8oa,b
9	41°21' 80"	32° 66' 13"	S9na,b	W9na,b	9	41° 14' 37"	32°41' 39	S9oa,b	W9oa,b
10	41°21' 86"	32° 66' 19"	S10na,b	W10na,b	10	41° 12' 16"	32°37' 47"	S10oa,b	W10oa,b
11	41° 23' 07"	32° 66' 52"	S11na,b	W11na,b					
12	41° 13' 55"	32° 40' 07"	S12na,b	W12na,b					
13	41° 14' 10"	32° 40' 45"	S13na,b	W13na,b					
14	41° 15' 04"	32° 40' 46"	S14na,b	W14na,b					
15	41° 12' 14"	32° 37' 32"	S15na,b	W15na,b					

The detectors were collected after a period of exposure, then detectors were transferred to a chemical etching process, then we calculating tracks density using an optical microscope after comparing it with the standard to get the radon concentraion.

4.2.2. Etched Solution

Alkaline solutions, including NaOH, KOH and various chemical additions such (ethanol), are used to etch areas of damage and reveal residues on plastic materials. In a Bottle volumetric container with a capacity of (0.25) liter, we utilized white, spherical granules of sodium hydroxide (NaOH), that had been dissolved in distilled water, in order to etching the detectors after the solution has reached thermal equilibrium. The granules of sodium hydroxide as shown in Figure (3.2).

Figure 2.2. The coordinates of the residential sites and their symbols

4.3. DEVICES AND TOOLS

4.3.1. Water Bath

The water bath type (UYM1S4) made by Metu Elektrometanik / Turkey was used to heat water inside then the etched solution (NaOH). This tool has a thermometer that control the temperature with an accuracy of (±1ºC) with the range of (0-100ºC), as shown in Figure (3.3).

Figure 3.3. Water bath.

4.3.2. Optical microscope

To calculate the tracks density a Chinese-made light microscope (Novel) was used. It has four objective lenses with the following magnification powers: 100X, 40X, 20X, and 10X. The 40X eyepiece has been apply. In addition, it contains two lenses with the ability to measure the area and the diameter of track. Figure (3.4) show the light microscope used in this work.

Figure 4.4. Optical microscope.

4.3.3. Sensitive Balance

A sensitive balance type Denver instrument MXX-612 model, a Canadian-made used to determine the mass of sodium hydroxide (NaOH) crystals with ±0.01 g. Figure (3-5) shows sensitive balance.

Figure 5.5. The sensitive balance.

4.4. EXPERIMENTAL PART

4.4.1. Preparation of Etching Solution

The etched solution (NaOH), which we produce from sodium hydroxide, created a normality of (6.25mol/L). The NaOH granules were dissolved in an amount of (62.5gm) in (0.25) liter of distilled water, where a volumetric bottle was used to dissolve the granules in it. It must be remember that the water level inside the bottle is low because, it decreases due to the high temperature that evaporate the solution. So water added after the solution is get thermal equilibrium with the surroundings.

Using the following equation, the weight of the sodium hydroxide granules determined.

$$W(gm) = N \times V_w \times W_{eq} \quad (3.1)$$

The (W_{eq}) represents the molecular weight of (NaOH) calculated as following:

$$W_{eq} = m\,(Na) + m(O) + m(H) \quad (3.2)$$

$$W_{eq} = 22.98977 + 15.9994 + 1.00794 = 39.99711\ gm\backslash mole$$

Where m is the mass of the elements. The required volume of distilled water is (1/4) liter.

The required molarity N is (6.25 mole\L).

W(gm), the weight of the sodium hydroxide granules, and by substituting the above numbers, we find.

W(gm) = 6.25 mole\L × 0.25× 40gm\mole = 62.5 (gm)

4.4.2. Chemical Etching

The chemical etching procedure was performed using a sodium hydroxide (NaOH) solution with Normality of (6.25 mole/L), where this etching solution was placed In a glass beaker inside the water bath that was heated to (60^{o}C). The CR-39 detector suspended by a copper wire inside the conical glass beaker placed in the bath for six hours with. After finishing the chemical etching procedure, the detectors carried to be wash with distilled water and dried. The concentration of the etching solution also altered throughout this process. The etching method shown in Figure (3.6).

Figure 6.6. Shows the chemical skimming process for the CR-39 nuclear trace detector.

4.4.3. Determination of Radon Concentration

After the detectors have dried, the number of tracks per unit area (track density ρ) counted by using a light microscope with magnification of (400X) using a calibration lens that is divided into several squares figure (3.7), and calculating the area of square A before calculating the number of traces per unit area (10 attempts are made for each detector). According to equation (3.3), the density of tracks calculated by dividing the average (N_{avg}) for each detector by the square's area.

$$\boldsymbol{\rho} = \frac{\mathrm{Navg}}{A} \tag{3.3}$$

Where ρ is the density of tracks (Track \mm^2)

N_{avg} the average counts for ten attempts.

The area of the large square in the calibration lens is 0.07 mm^2.

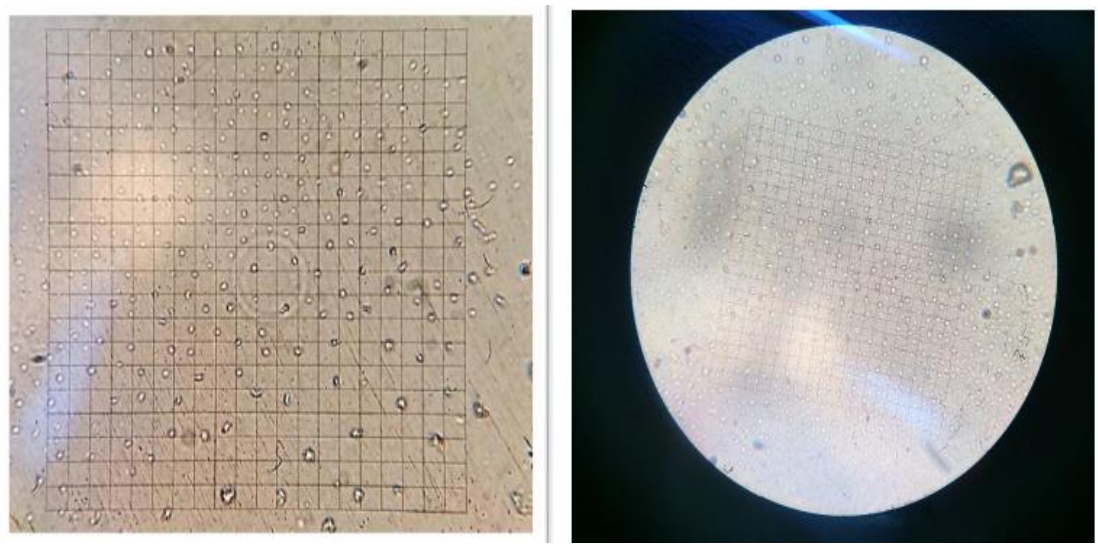

Figure 7.7. Shows the traces of alpha particles in the (CR-39) detector.

The concentration of radon in the air expressed in Bq/m^3, and the following equation used to calculate radon concentration:

$$C_{Rn}=E_s/\rho_s(\rho/t)= (\rho/t)\ 1/k \quad (3.4)$$

Where, ρ the track density (number of tracks / mm^2), t: the exposure time (days), E_s: the radon exposure of the standard source ($Bq.day.m^{-3}$), and ρ_s: the track density of the standard source, *k* is the calibration factor is equal to (0.169 $track.m^2/Bq.day.mm^2$) as in figure (3.8). This work done by supervisor in Baghdad University / college of Education for pure Sciences / Ibn Al- Haithem.

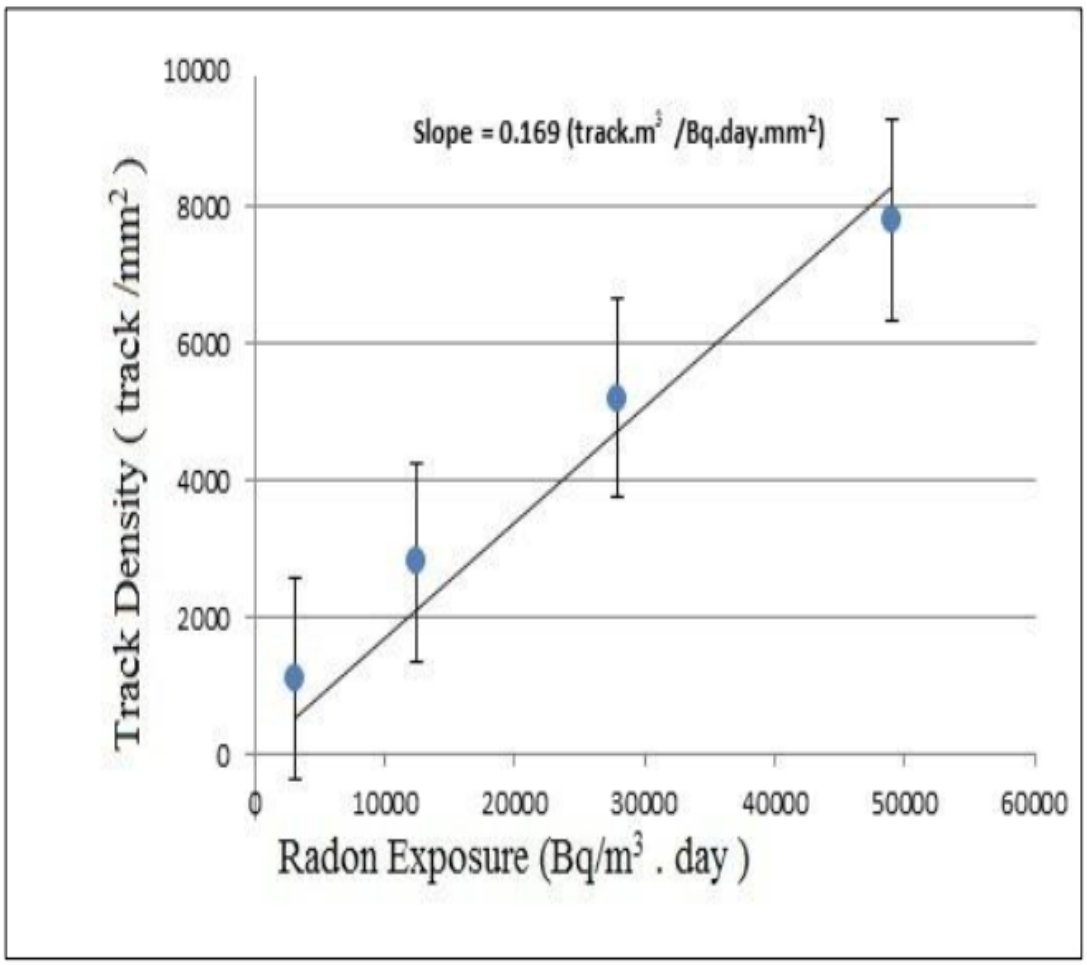

Figure 8.8. Calibration line for slandered sample.

PART 5

PREFACE

This chapter includes a show and discussion of the results of radon concentrations for two seasons inside Karabuk buildings using CR-39 detector. The first season (from July to August of the same year) and the second (from February to March of the following year).

5.1. RESULTS AND DISCUSSION

Following the installation of solid-state nuclear trace detectors CR-39 in the chosen Karabük buildings, the detectors were distributed and collected. The radon gas concentrations then determined by calibration by comparing the results to slandered sample. Using the relationships (3.5) and (3.6), radon gas concentrations calculated for the samples using the relationship between the intensity of traces and radon exposure to the standard source, where the relationship was linear as shown in Figure (3.15) and from the slope of the graph. The results of the radon gas concentrations, the intensity of traces, and radioactive indicators for the season were included. Table

5.1.1. Radon Gas Concentration First Season (Summer)

Table (2) present the concentrations of radon gas in the air with the density of tracks, which is an indicator for radioactivity within 100-yill buildings. The lowest concentration value on the first floor was around (34.846) Bq/m^3 for sample (S10ob), which is the lowest value recorded for this season. As for the highest value of radon gas concentration on the ground floor, was around (60.487) Bq/m^3 for the sample (S30a). The reason for the decrease in radon gas concentrations in the summer is continuous ventilation in homes by constantly opening the windows, as well as the

using of building material of construction they may contain a small number of radioactive materials.

During the summer, the S4nb sample had the heights radon gas concentration of 51.282 Bq/m^3 and the lowest concentration of 30.901 Bq/m^3 in modern residential dwellings sample S8nb.

Additionally, the strength of the effects and radiological indices (AED (mSv/y), LCR (WLM) per 10^6 persons, PAEC (mWL), D_{soft} (nGy/h), D_{lung} (nGy/h), H_{eff} (nSv/h)) are shown together with the radon gas concentrations in Tables (2,3).

5.1.2. Radon Gas Concentration in Second Season (Winter)

Table 4 shows the heights radon concentrations were in sample (W3oa) was (113.084 Bq/m^3) and lowest in samples (W5oa) was (82.183 Bq/m^3) during the winter and in older dwellings.

Table 5 shows that the highest radon concentration in the modern residential homes for the winter season was (77.581 Bq/m^3) in sample (W1na), and the lowest concentration was (55.834 Bq/m^3) in sample (W2na).

Additionally, the strength of the effects and radiological indices (AED (mSv/y), LCR (WLM) per 10^6 persons, PAEC (mWL), D_{soft} (nGy/h), D_{lung} (nGy/h), H_{eff} (nSv/h)) are shown together with the radon gas concentrations in Tables (4,5).

The results of radon concentrations in the four tables (4.2-4.5), indicate that an increasing of 52.78% in the old residential floors more than the radon concentrations in modern residential floors in the winter season. In summer, the increase rate was 39.78% in the old residential than the radon concentrations in modern residential, and this increase of radon is due to more than one reason, that including:

First, the main reason, as it is known and proven in scientific researches, the internal ventilation, which is due to the design of the residential floors. We find that the old

ones have little ventilation due to the nature of the cold weather, as most of their walls consist of small windows, while we find the modern ones with large windows that can occupy 30 % of the building.

Secondly, the use of more building materials in the abutments and partitions of the old houses, and this, as is well known, contributes to building materials that lead to an effective increase in radon concentration because they contain uranium.

Thirdly, since radon is one of the daughters of uranium, which is present in the earth's crust, so we find that the concentration of radon varies from one region to another. Accordingly, we need more information about this role and its specifications, in addition to the latest information about radioactivity in the surface soil, and the type of building materials, for the purpose of identifying the real causes that contribute to the increase in radon concentration and working to reduce its impact.

The Health Physics Department of the Cekmece Nuclear Research and Training Centre (CNAEM) was the first how start working with internal radon measurements in Turkey. start in 1984, until 2007 published their data about their work[104]. The work included 53 provinces in addition to the work done by Koksal in 1993, Gurel and Cobanoglu 1997[83], these studies did not include Karabuk governorate, except the study done by Celebi and Ulug, 2002[84], which did not follow the comparison approach between the old and modern residential homes for the summer and winter seasons. Table 5 shows the most important results of local studies. As for Table No. 6, shows some results of the internal radon concentration of some countries near and far from Turkey, where the results of this work can be compared with the results mentioned in the two tables, which show their compatibility with the local results, and their closeness to the results of nearby countries with close geological formation.

The tables 1,2,3, and 4 also showed that radiation indices AED (mSv/y), LCR (WLM) per 106 persons, PAEC (mWL), D_{soft} (nGy/h), D_{lung} (nGy/h), and H_{eff} (nSv/h) ranged (1.140-2.853), ($4.15x10^{-2}$-$8.39x10^{-2}$), (0.006797-0.013753), (0.279-0.411), (2.235-3.287), and (10.059-14.793) respectively for winter season, and (0.783-1.543),($2.29x10^{-2}$-$4.54x10^{-2}$), (0.003758-0.007436), (0.155-0.306), (1.236-2.446),

(5.562-11.006) for summer season. All these results less than the values recommended by the international agencies UNSCEAR, WHO&ICRP [83], [85], [86]

Table 5.1. Radon concentrations and their indices for old residential in the summer season.

s.no	Track density (ρ) (track/mm^2)	Rn conc. (C_{Rn}) (Bq/m^3)	AED (mSv/y)	LCR (WLM) per 10^6 persons	PAEC (mWL)	D_{soft} (nGy/h)	D_{lung} (nGy/h)	H_{eff} (nSv/h)
S1oa	900	59.172	1.492828	4.39E-02	0.007197	0.296	2.367	10.651
S1ob	800	52.597	1.326959	3.9E-02	0.006397	0.263	2.104	9.467
S2oa	930	61.144	1.542589	4.54E-02	0.007436	0.306	2.446	11.006
S2ob	790	51.940	1.310372	3.85E-02	0.006317	0.260	2.078	9.349
S3oa	920	60.487	1.526002	4.49E-02	0.007356	0.302	2.419	10.888
S3ob	900	59.172	1.492828	4.39E-02	0.007197	0.296	2.367	10.651
S4oa	810	53.254	1.343546	3.95E-02	0.006477	0.266	2.130	9.586
S4ob	890	58.514	1.476241	4.34E-02	0.007117	0.293	2.341	10.532
S5oa	770	50.625	1.277198	3.76E-02	0.006157	0.253	2.025	9.112
S5ob	810	53.254	1.343546	3.95E-02	0.006477	0.266	2.130	9.586
S6oa	740	48.652	1.227437	3.61E-02	0.005917	0.243	1.946	8.757
S6ob	730	47.995	1.21085	3.56E-02	0.005837	0.240	1.920	8.639
S7oa	770	50.625	1.277198	3.76E-02	0.006157	0.253	2.025	9.112
S7ob	780	51.282	1.293785	3.8E-02	0.006237	0.256	2.051	9.231
S8oa	770	50.625	1.277198	3.76E-02	0.006157	0.253	2.025	9.112
S8ob	730	47.995	1.21085	3.56E-02	0.005837	0.240	1.920	8.639
S9oa	790	51.940	1.310372	3.85E-02	0.006317	0.260	2.078	9.349
S9ob	730	47.995	1.21085	3.56E-02	0.005837	0.240	1.920	8.639
S10oa	530	34.846	1.094741	3.22E-02	0.005277	0.217	1.736	7.811
S10ob	530	34.846	0.87911	2.58E-02	0.004238	0.174	1.394	6.272
Global limit	-	200 - 300 (Bq/m3) [20]	3-10 (mSv/y) [18]	170-230 [8]	-	-	-	3-10 mSv.y-1 [17]

Table 5.2. Radon concentrations and it`s indices for new residential in summer season.

s.no	track density (ρ) (track/mm^2)	Rn conc. (C_{Rn}) (Bq/m^3)	AED (mSv/y)	LCR (WLM) per 10^6 persons	PAEC (mWL)	D_{soft} (nGy/h)	D_{lung} (nGy/h)	H_{eff} (nSv/h)
S1na	500	32.873	0.829349	2.44E-02	0.003998	0.164	1.315	5.917
S1nb	540	35.503	0.895697	2.63E-02	0.004318	0.178	1.420	6.391
S2na	530	34.846	0.87911	2.58E-02	0.004238	0.174	1.394	6.272
S2nb	600	39.448	0.995219	2.93E-02	0.004798	0.197	1.578	7.101
S3na	570	37.475	0.945458	2.78E-02	0.004558	0.187	1.500	6.746
S3nb	640	42.079	1.061567	3.12E-02	0.005118	0.210	1.683	7.574
S4na	680	44.707	1.127915	3.32E-02	0.005437	0.224	1.788	8.048
S4nb	780	51.282	1.293785	3.8E-02	0.006237	0.256	2.051	9.231
S5na	650	42.735	1.078154	3.17E-02	0.005198	0.214	1.709	7.692
S5nb	760	49.967	1.260611	3.71E-02	0.006077	0.250	1.999	8.994
S6na	580	38.133	0.962045	2.83E-02	0.004638	0.191	1.525	6.864
S6nb	630	41.420	1.04498	3.07E-02	0.005038	0.207	1.657	7.456
S7na	600	39.448	0.995219	2.93E-02	0.004798	0.197	1.578	7.101
S7nb	630	41.420	1.04498	3.07E-02	0.005038	0.207	1.657	7.456
S8na	720	47.337	1.194263	3.51E-02	0.005757	0.237	1.893	8.521
S8nb	470	30.901	0.779588	2.29E-02	0.003758	0.155	1.236	5.562
S9na	570	37.475	0.945458	2.78E-02	0.004558	0.187	1.499	6.746
S9nb	550	36.160	0.912284	2.68E-02	0.004398	0.181	1.446	6.509
S10na	580	38.133	0.962045	2.83E-02	0.004638	0.191	1.525	6.864
S10nb	640	42.078	1.061567	3.12E-02	0.005118	0.210	1.683	7.574
S11na	590	38.790	0.978632	2.88E-02	0.004718	0.194	1.552	6.982
Global limit	-	200 - 300 (Bq/m3) [20]	3-10 (mSv/y) [18]	170-230 [8]	-	-	-	3-10 mSv.y-1 [17]

Table 5.3. Radon concentrations and it`s indices for old residential in winter season.

s.no	track density (ρ) (track/mm^2)	Rn conc. (C_{Rn}) (Bq/m^3)	AED (mSv/y)	LCR (WLM) per 10^6 persons	PAEC (mWL)	D_{soft} (nGy/h)	D_{lung} (nGy/h)	H_{eff} (nSv/h)
W1oa	1500	98.619	2.488047	7.32E-02	0.011994	0.493	3.945	17.751
W1ob	1530	100.592	2.537808	7.46E-02	0.012234	0.503	4.024	18.107
W2oa	1270	83.498	2.106547	6.19E-02	0.010155	0.417	3.340	15.030
W2ob	1430	94.017	2.371938	6.97E-02	0.011435	0.470	3.761	16.923
W3oa	1720	113.084	2.852961	8.39E-02	0.013753	0.565	4.523	20.355
W3ob	1670	109.796	2.770026	8.14E-02	0.013354	0.549	4.392	19.763
W4oa	1550	101.907	2.570982	7.56E-02	0.012394	0.510	4.076	18.343
W4ob	1400	92.045	2.322178	6.83E-02	0.011195	0.460	3.682	16.568
W5oa	1250	82.183	2.073373	6.1E-02	0.009995	0.411	3.287	14.793
W5ob	1330	87.442	2.206069	6.49E-02	0.010635	0.437	3.498	15.740
W6oa	1520	99.934	2.521221	7.41E-02	0.012154	0.500	3.997	17.988
W6ob	1620	106.509	2.687091	7.9E-02	0.012954	0.533	4.260	19.172
W7oa	1320	86.785	2.189482	6.44E-02	0.010555	0.434	3.471	15.621
W7ob	1590	104.537	2.63733	7.75E-02	0.012714	0.523	4.181	18.817
W8oa	1440	94.6746	2.388525	7.02E-02	0.011514	0.473	3.787	17.041
W8ob	1260	82.840	2.08996	6.14E-02	0.010075	0.414	3.314	14.911
W9oa	1390	91.387	2.305591	6.78E-02	0.011115	0.457	3.655	16.450
W9ob	1500	98.619	2.488047	7.32E-02	0.011994	0.493	3.945	17.751
W10oa	1540	101.249	2.554395	7.51E-02	0.012314	0.506	4.050	18.225
W10ob	1500	98.619	2.488047	7.32E-02	0.011994	0.493	3.945	17.751
Global limit	-	200 - 300 (Bq/m3) [106]	3-10 (mSv/y) [104]	170-230 [8]	-	-	-	3-10 mSv.y-1 [17]

Table 5.4. Radon concentrations and it`s indices for new residential in winter season.

s.no	track density (ρ) (track/mm^2)	Rn conc. (C_{Rn}) (Bq/m^3)	AED (mSv/y)	LCR (WLM) per 10^6 persons	PAEC (mWL)	D_{soft} (nGy/h)	D_{lung} (nGy/h)	H_{eff} (nSv/h)
W1na	1180	77.581	1.957264	5.75E-02	0.009435	0.388	3.103	13.965
W1nb	960	63.116	1.59235	4.68E-02	0.007676	0.316	2.525	11.361
W2na	850	55.884	1.409893	4.15E-02	0.006797	0.279	2.235	10.059
W2nb	920	60.487	1.526002	4.49E-02	0.007356	0.302	2.419	10.888
W3na	940	61.801	1.559176	4.58E-02	0.007516	0.309	2.472	11.124
W3nb	920	60.487	1.526002	4.49E-02	0.007356	0.302	2.419	10.888
W4na	940	61.801	1.559176	4.58E-02	0.007516	0.309	2.472	11.124
W4nb	900	59.172	1.492828	4.39E-02	0.007197	0.296	2.367	10.651
W5na	870	57.199	1.443067	4.24E-02	0.006957	0.286	2.288	10.295
W5nb	990	65.089	1.642111	4.83E-02	0.007916	0.325	2.604	11.716
W6na	900	59.172	1.492828	4.39E-02	0.007197	0.296	2.367	10.651
W6nb	990	65.089	1.642111	4.83E-02	0.007916	0.325	2.604	11.716
W7na	930	61.144	1.542589	4.54E-02	0.007436	0.306	2.446	11.006
W7nb	980	64.431	1.625524	4.78E-02	0.007836	0.322	2.577	11.598
W8na	850	55.884	1.409893	4.15E-02	0.006797	0.279	2.235	10.059
W8nb	1080	71.006	1.791394	5.27E-02	0.008636	0.355	2.840	12.781
W9na	1060	69.691	1.75822	5.17E-02	0.008476	0.348	2.788	12.544
W9nb	1040	68.376	1.725046	5.07E-02	0.008316	0.342	2.735	12.308
W10na	930	61.144	1.542589	4.54E-02	0.007436	0.306	2.446	11.006
W10nb	960	63.116	1.59235	4.68E-02	0.007676	0.316	2.525	11.361
Global limit	-	200 - 300 (Bq/m3) [20]	3-10 (mSv/y) [18]	170-230 [8]	-	-	-	3-10 mSv.y-1 [17]

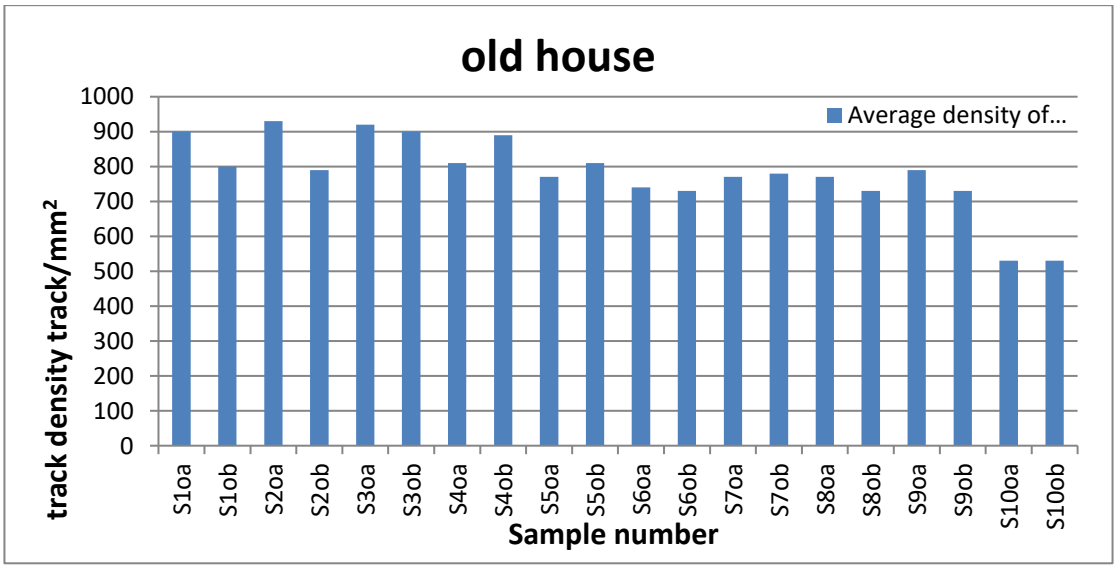

Figure 5.1. Average track density of radon gas for the summer season for old homes using the CR-39 nuclear trace detector.

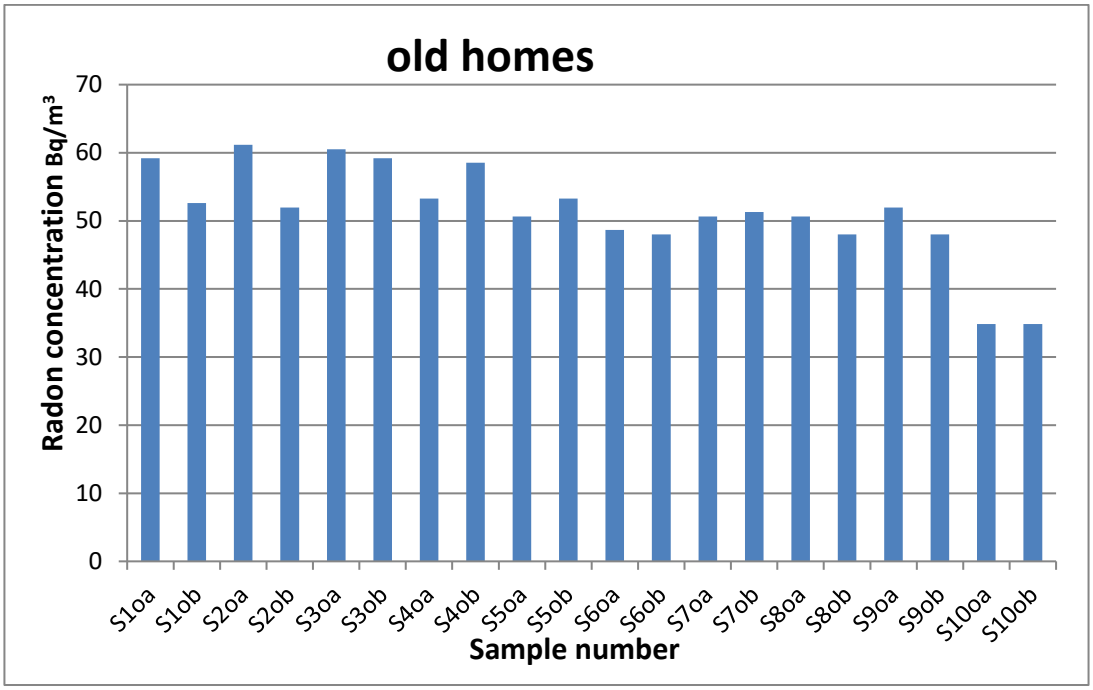

Figure 0.2. Radon gas concentration levels for the summer season for old houses using the CR-39 nuclear track detector.

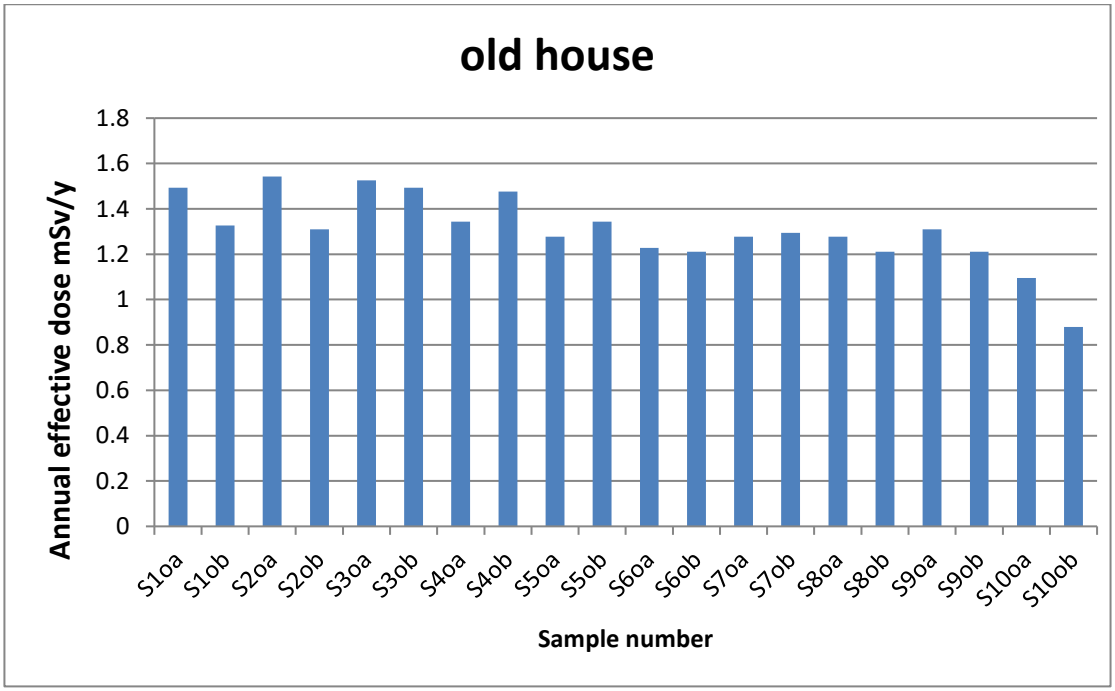

Figure 5.3. Annual effective dose for the summer season for old houses using the CR-39 nuclear trace detector.

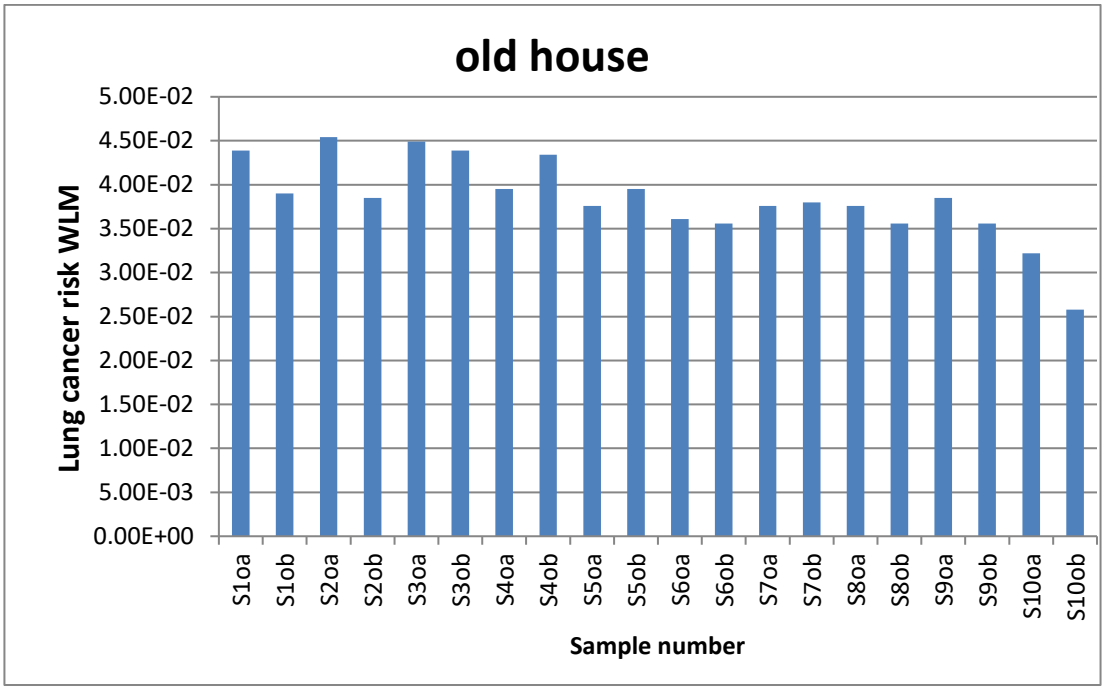

Figure 0.4. Lung cancer risk in the summer for old houses using the CR 39 nuclear pathway detector.

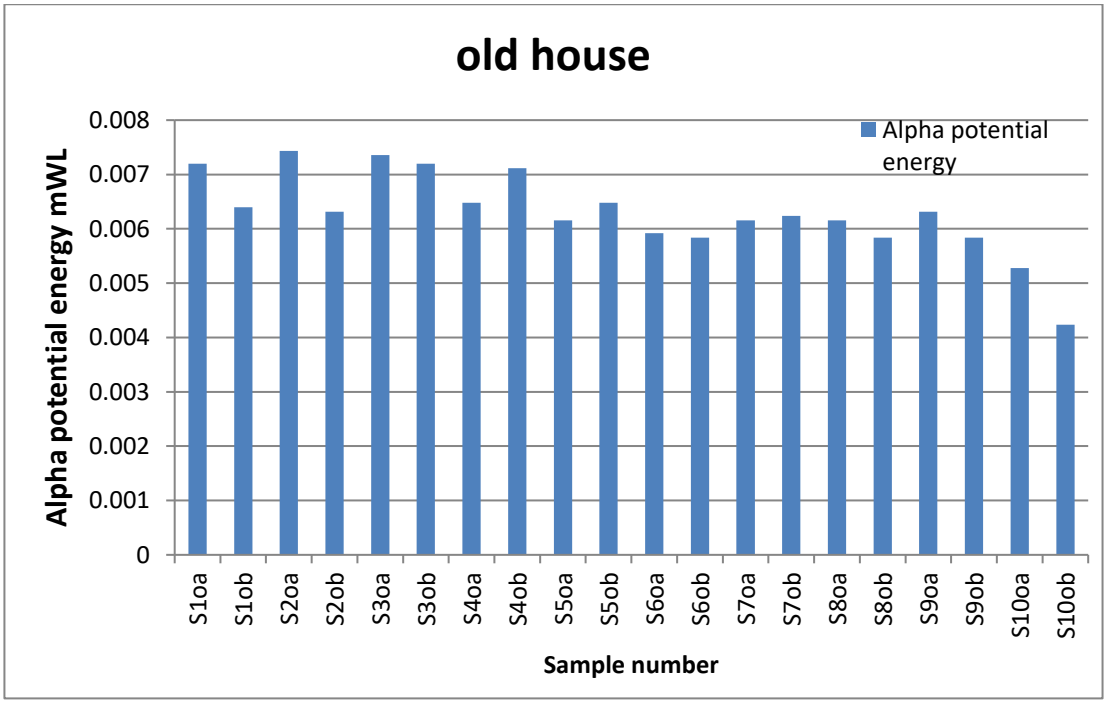

Figure 0.5. Alpha potential energy for the summer season of old houses using the CR 39 nuclear track detector.

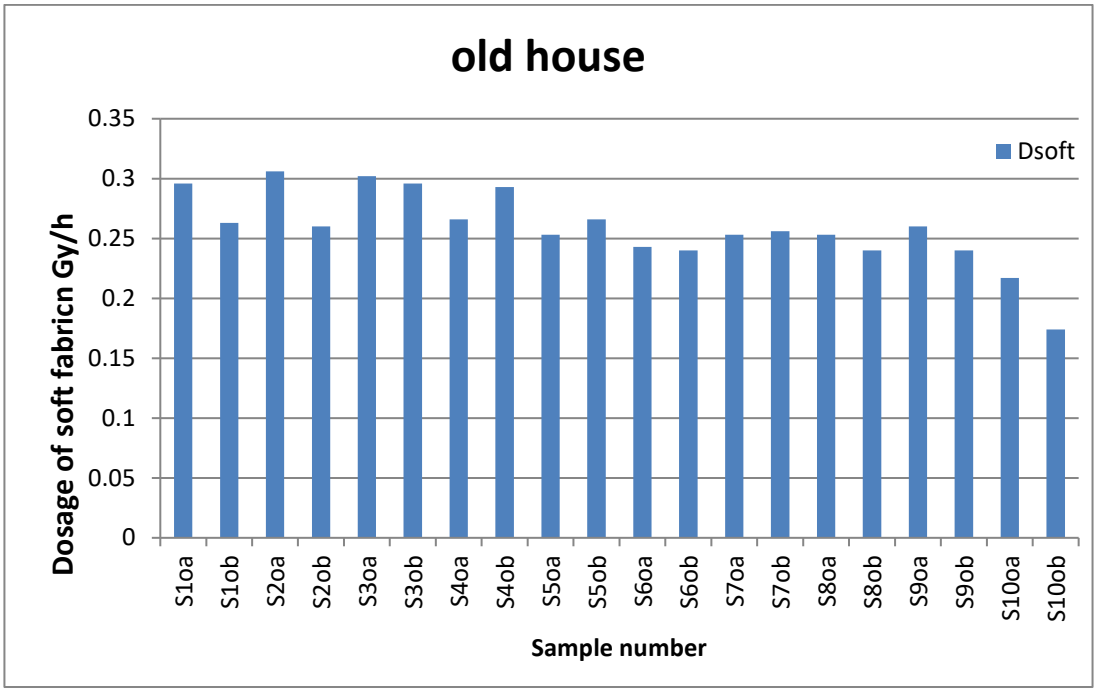

Figure 1.6. Dosage of soft fabric for wintering old houses using the CR-39 nuclear trace detector.

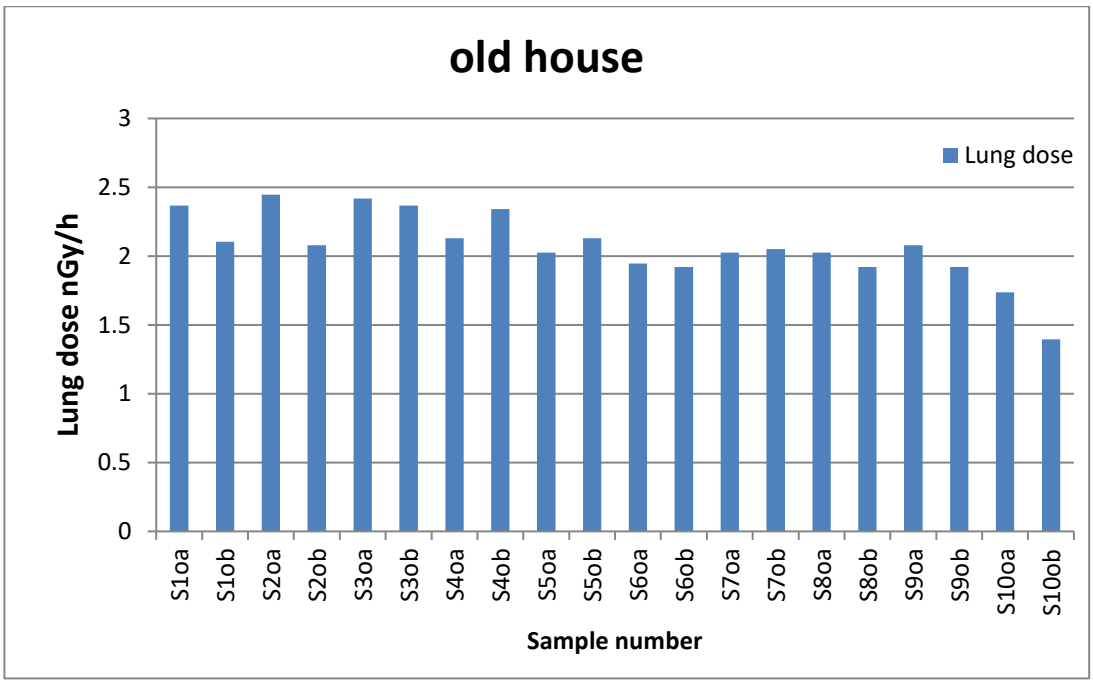

Figure 5.7. Lung dose for the summer season for old houses using the CR-39 nuclear trace detector.

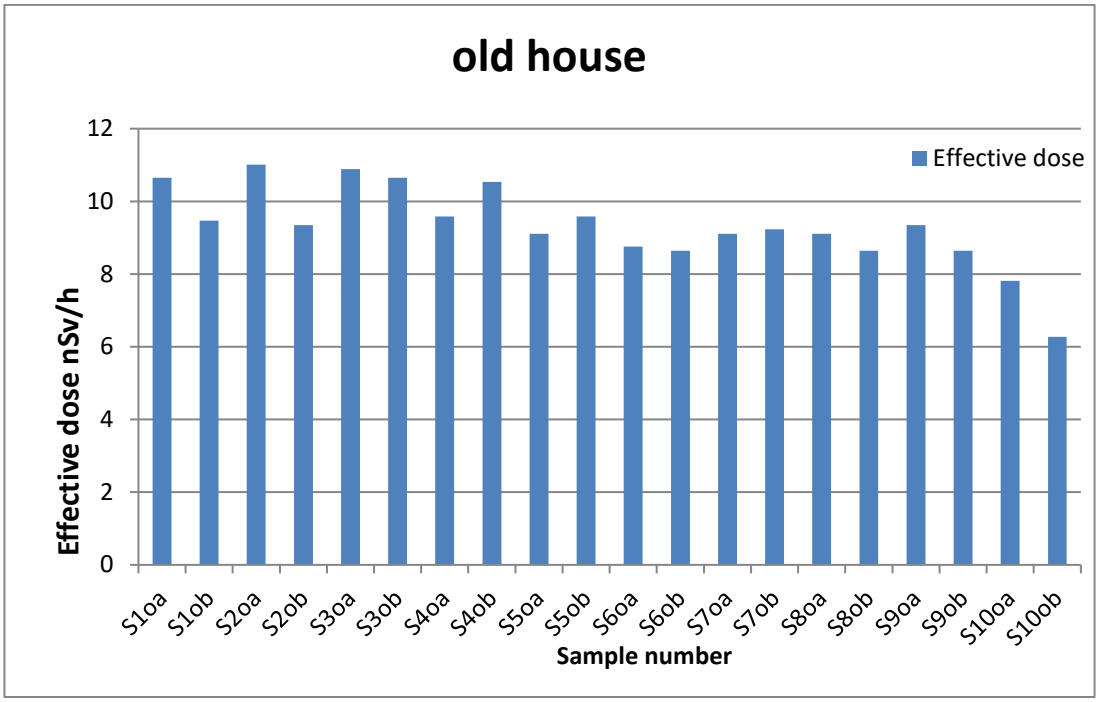

Figure 0.8. Effective dose for the summer season for old houses using the CR-39 nuclear trace detector.

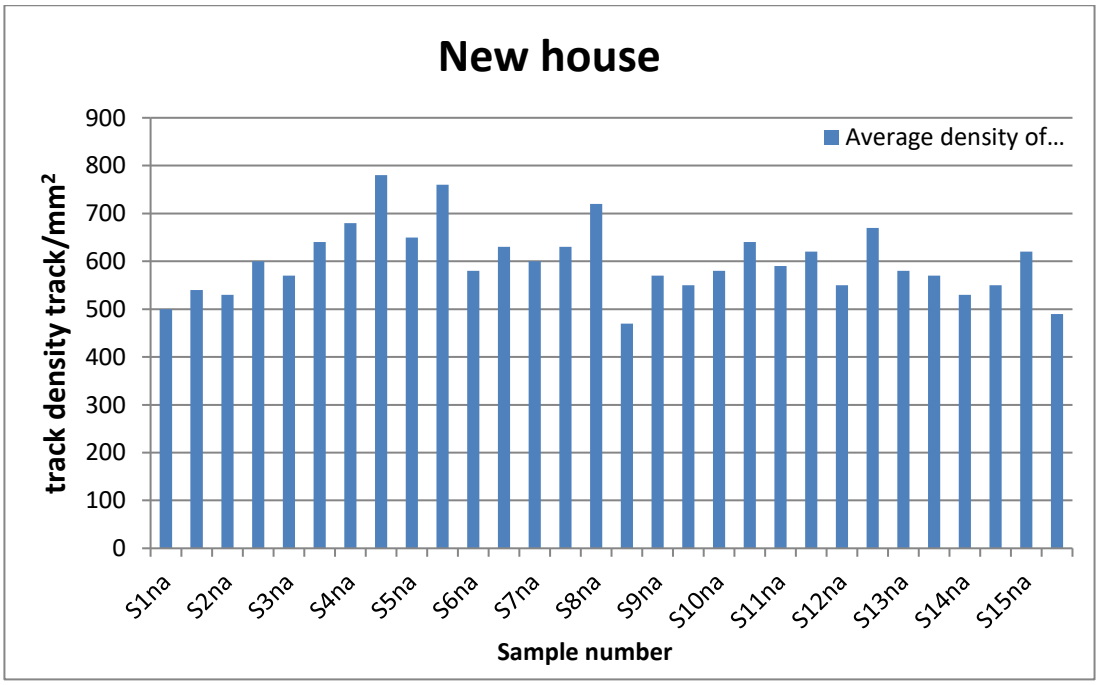

Figure 5.9. Average trace density of radon gas for the summer season for new houses using the CR-39 nuclear trace detector.

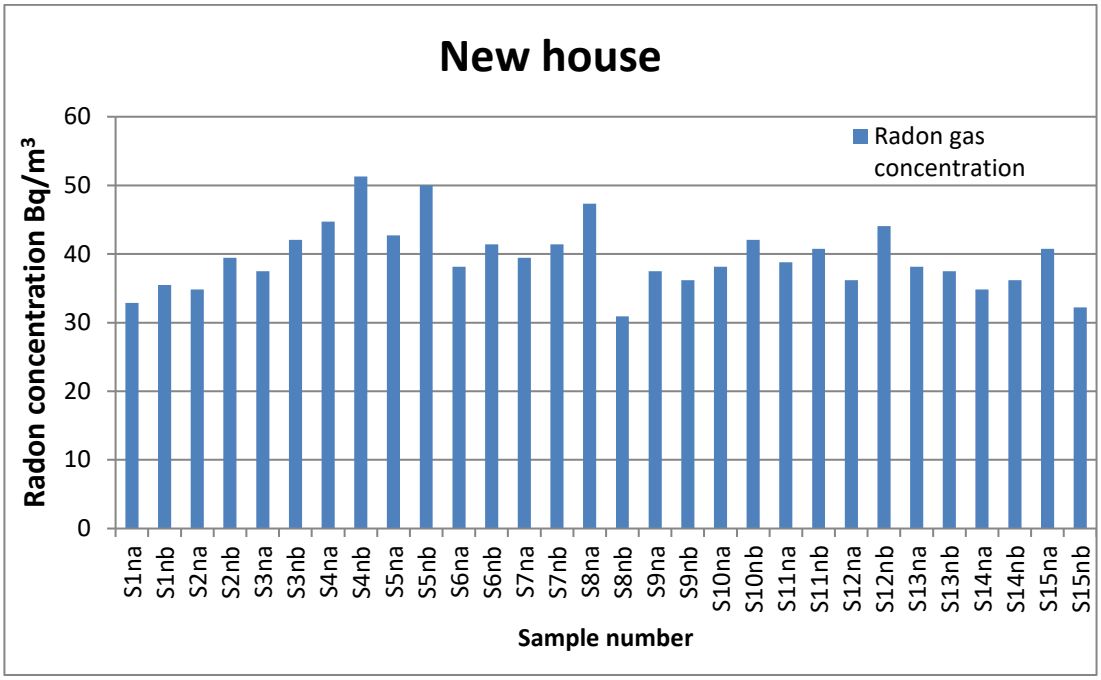

Figure 5.10. Radon gas concentration levels for the summer season for new houses using the CR-39 nuclear trace detector.

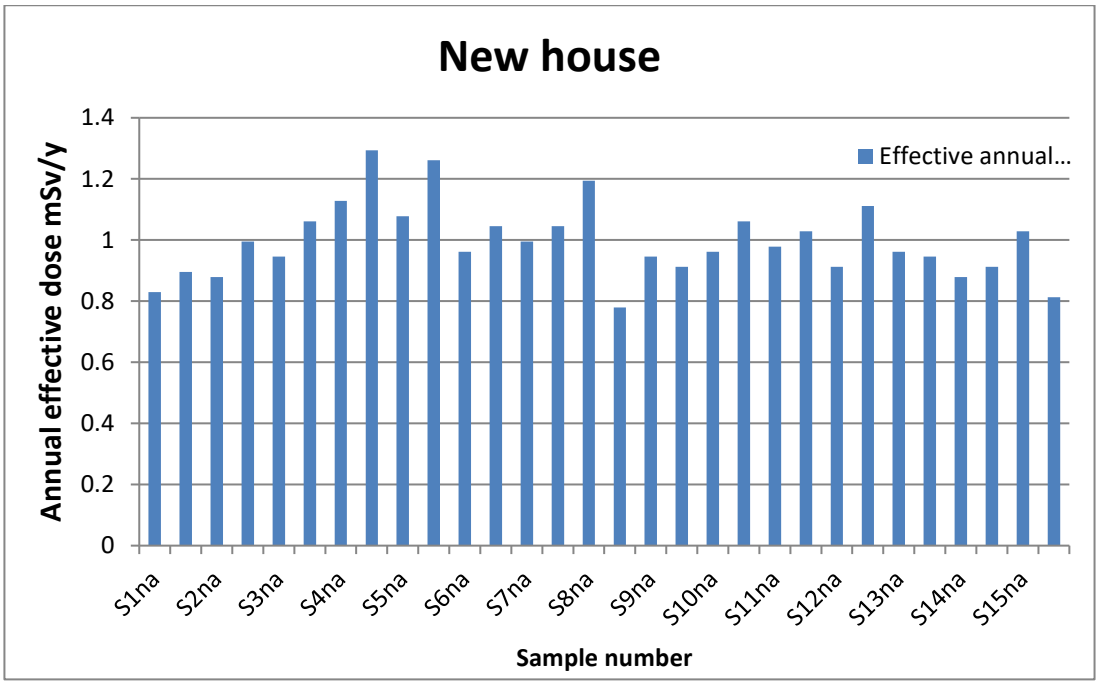

Figure 5.11. Annual effective dose for the summer season for new houses using the CR-39 nuclear trace detector.

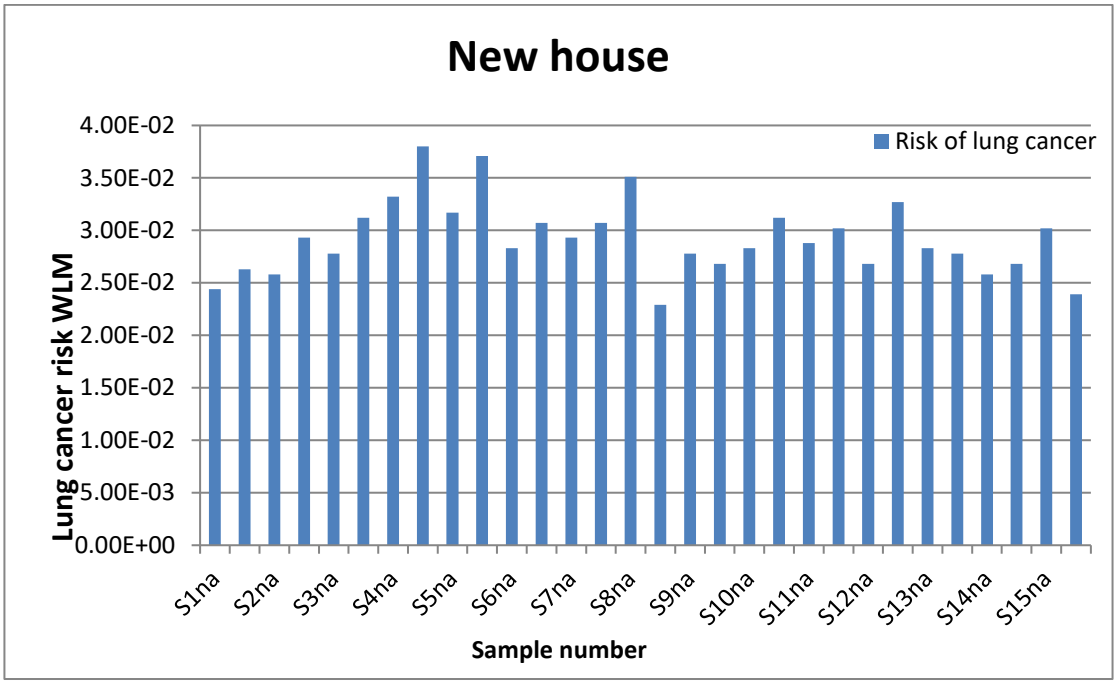

Figure 5.12. Lung cancer risk in the summer for new houses using the CR 39 nuclear pathway detector.

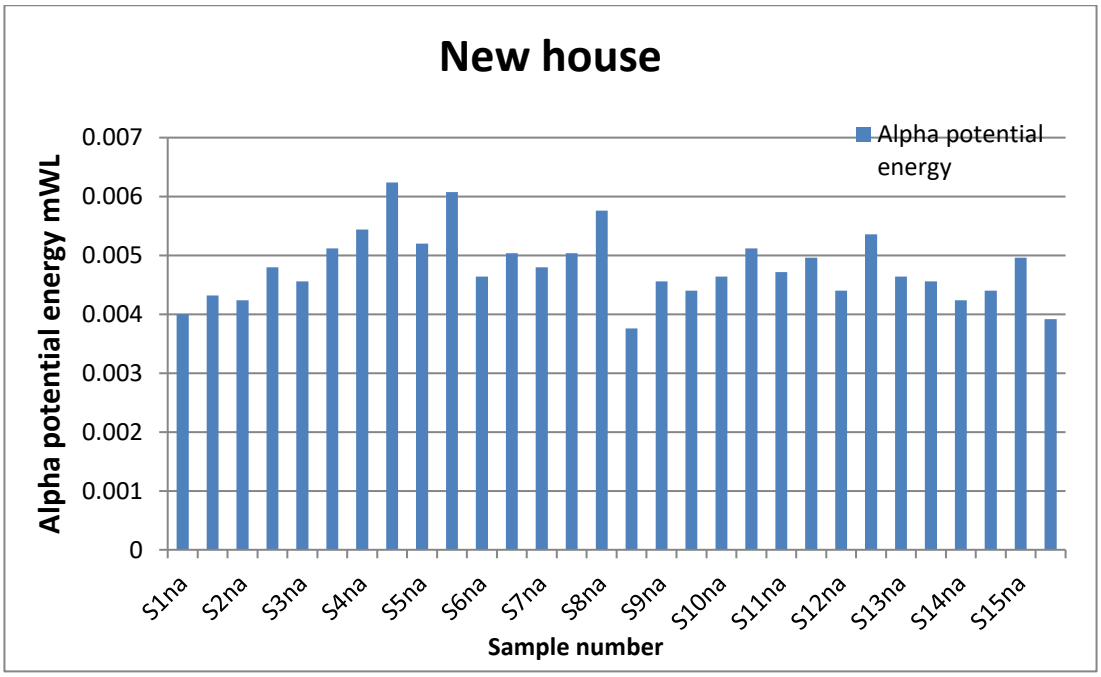

Figure 5.13. Alpha potential energy for the summer season of new houses using the CR 39 nuclear track detector.

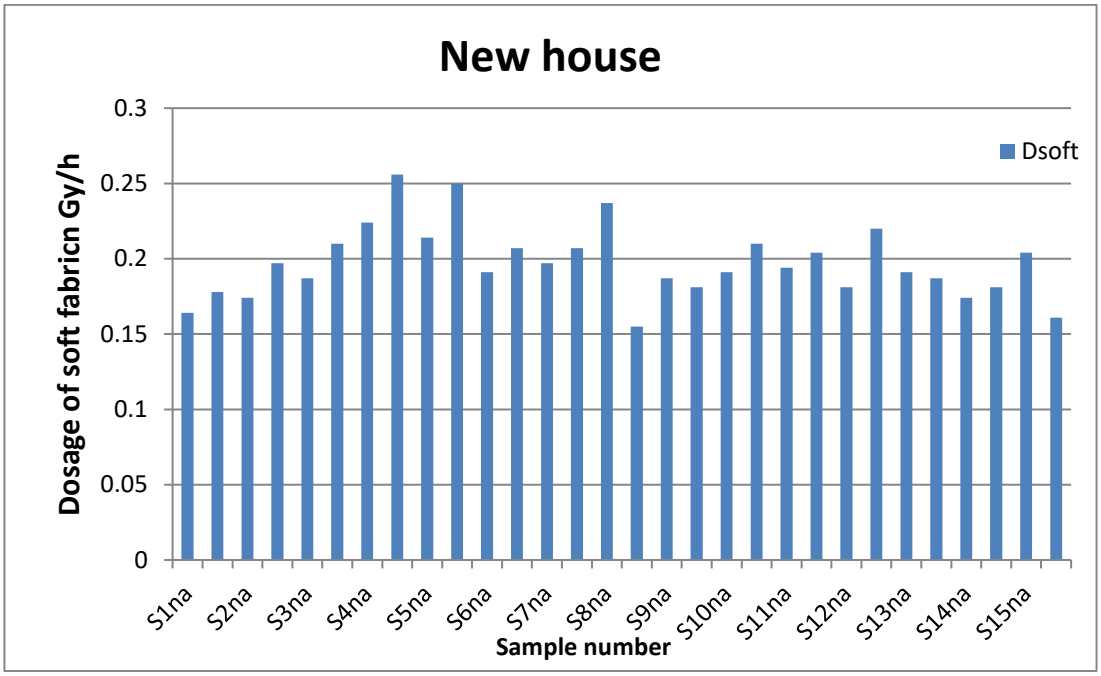

Figure 0.14. Dosage of soft fabric for wintering new houses using the CR-39 nuclear trace detector.

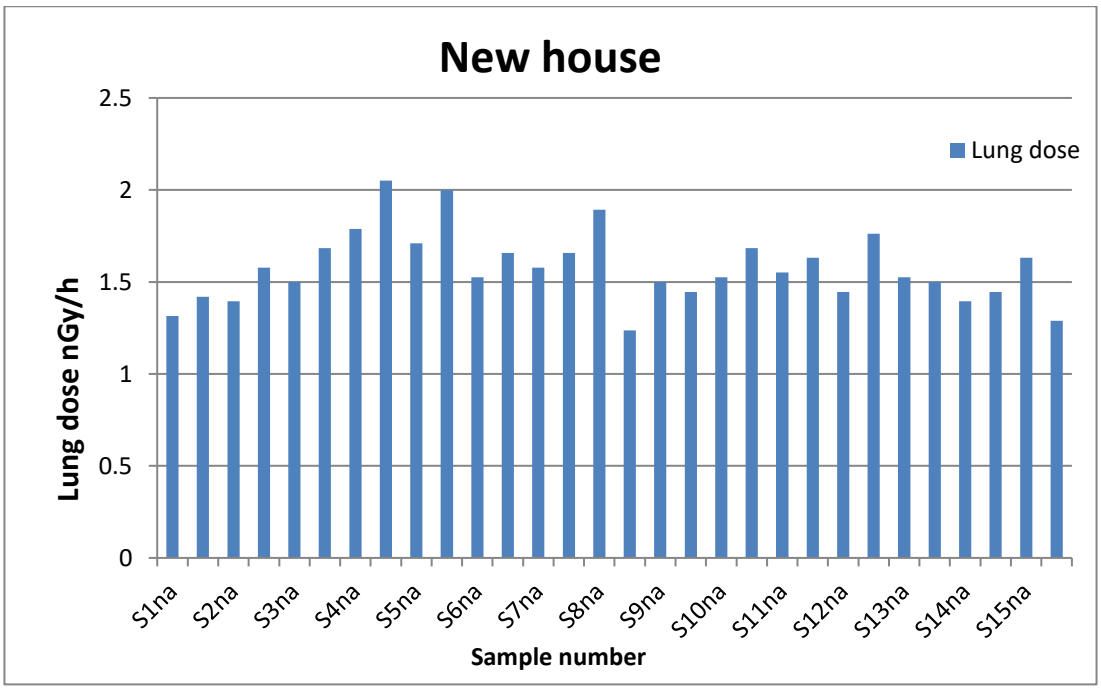

Figure 5.15. Lung dose for the summer season for new houses using the CR-39 nuclear trace detector.

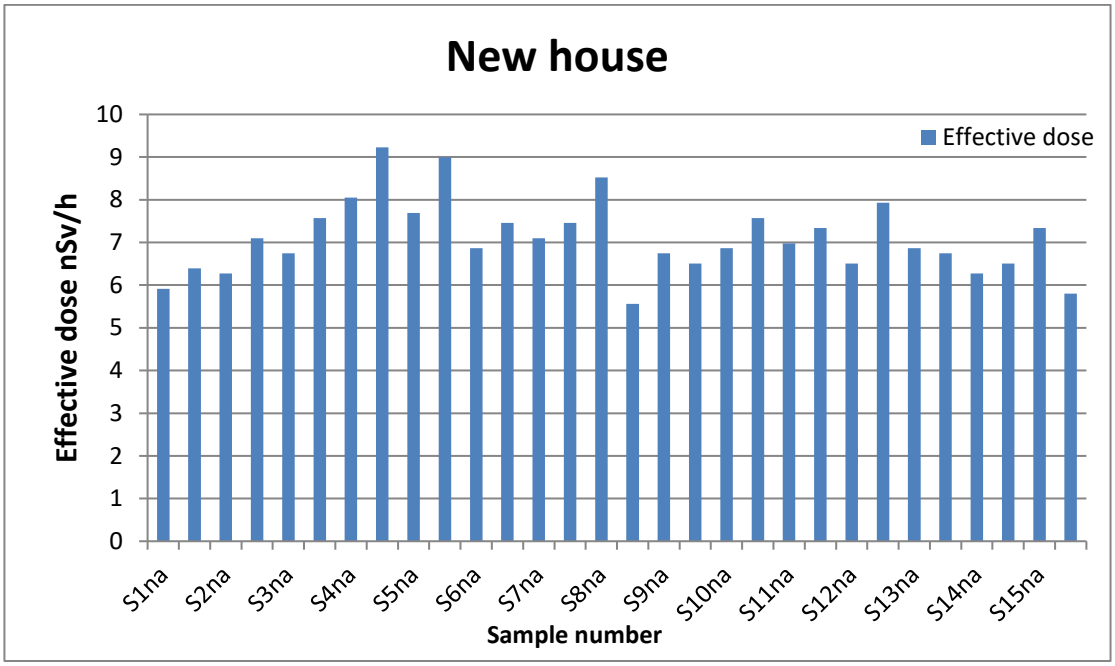

Figure 5.16. Effective dose for the summer season for new houses using the CR-39 nuclear trace detector.

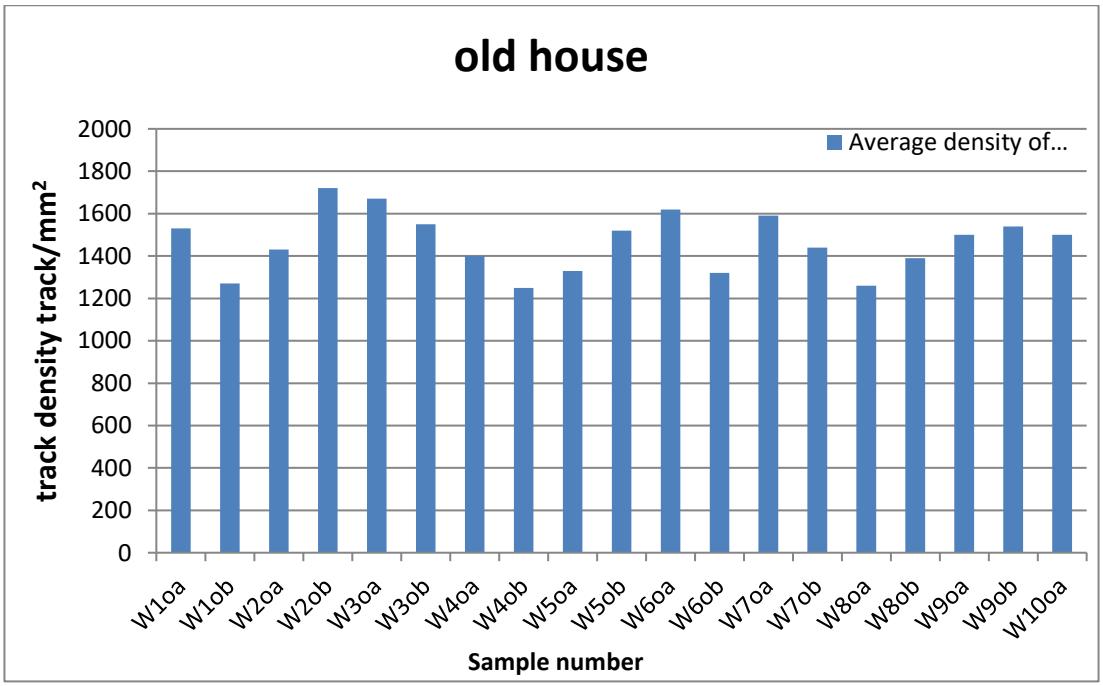

Figure 5.17. Average trace density of radon gas for the winter for old houses season using the CR-39 nuclear trace detector.

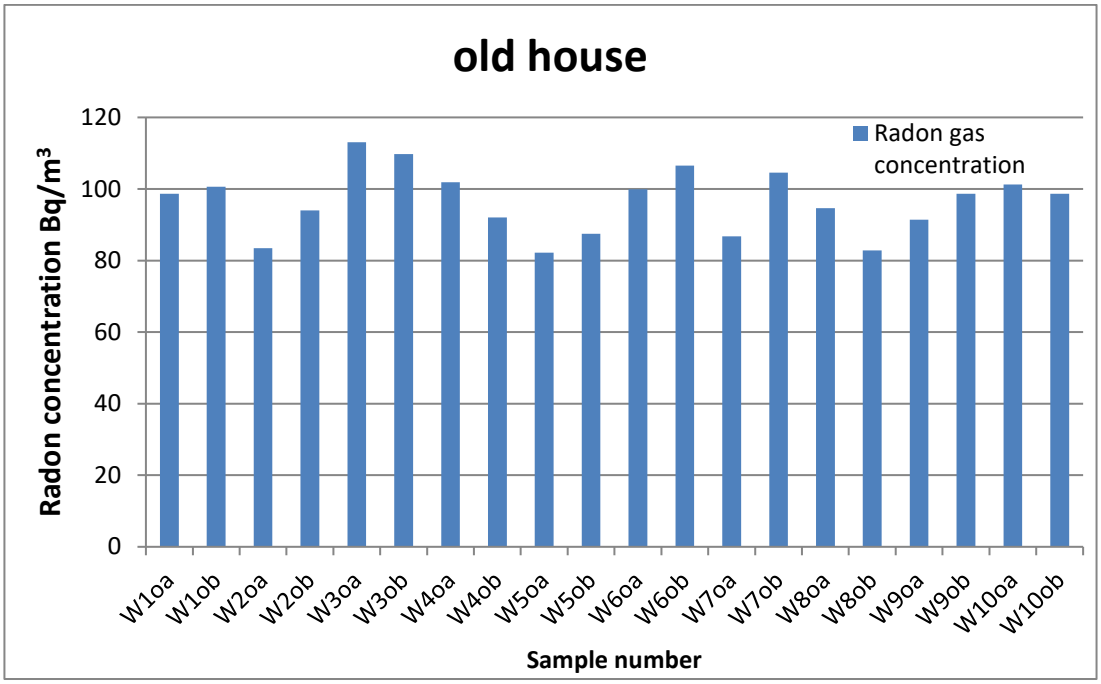

Figure 0.18. Levels of radon gas concentrations for the winter season for old houses using the CR-39 nuclear trace detector.

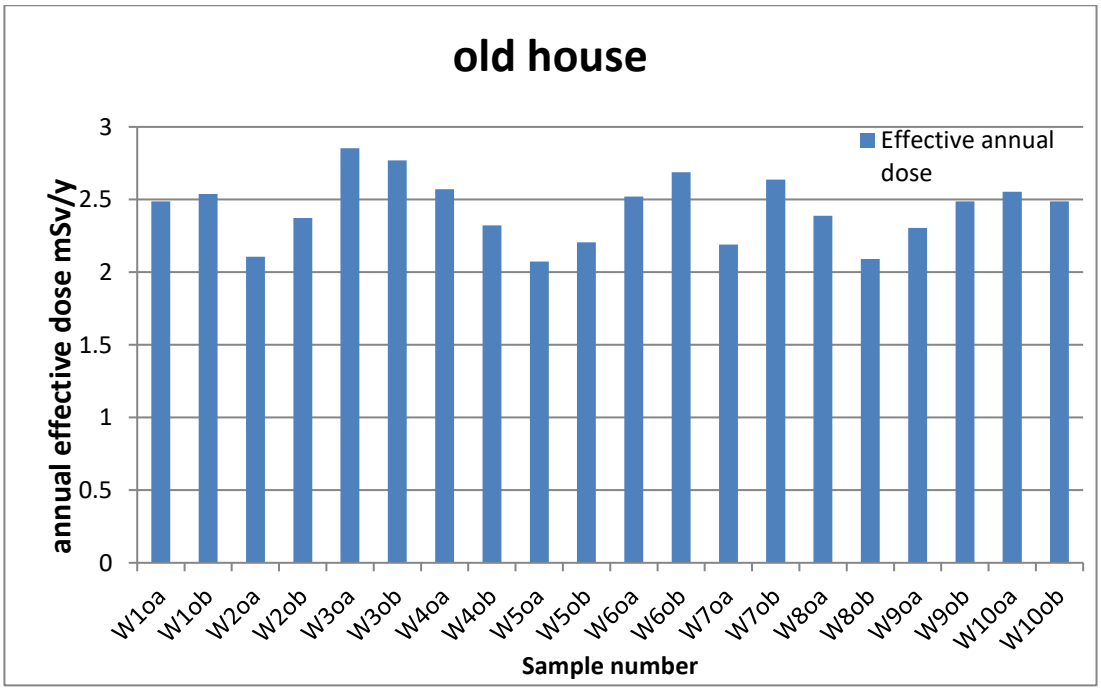

Figure 0.19. The annual effective dose for the winter season of old houses using the CR-39 nuclear trace detector.

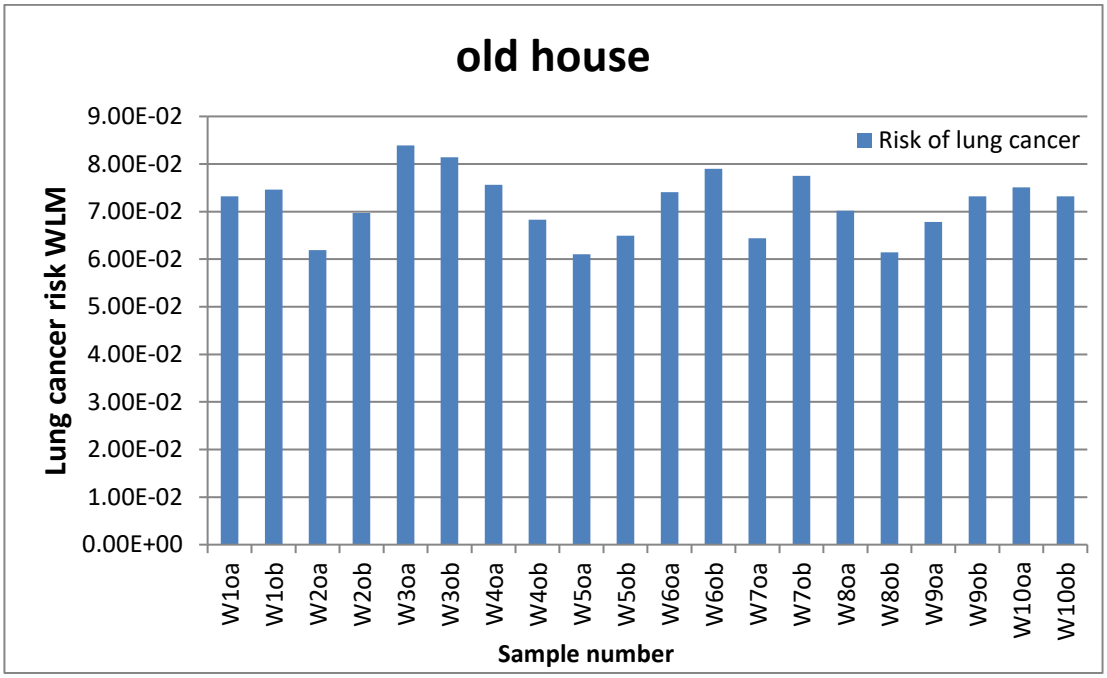

Figure 5.20. Risk of lung cancer for the winter season for old houses using the CR-39 nuclear trace detector.

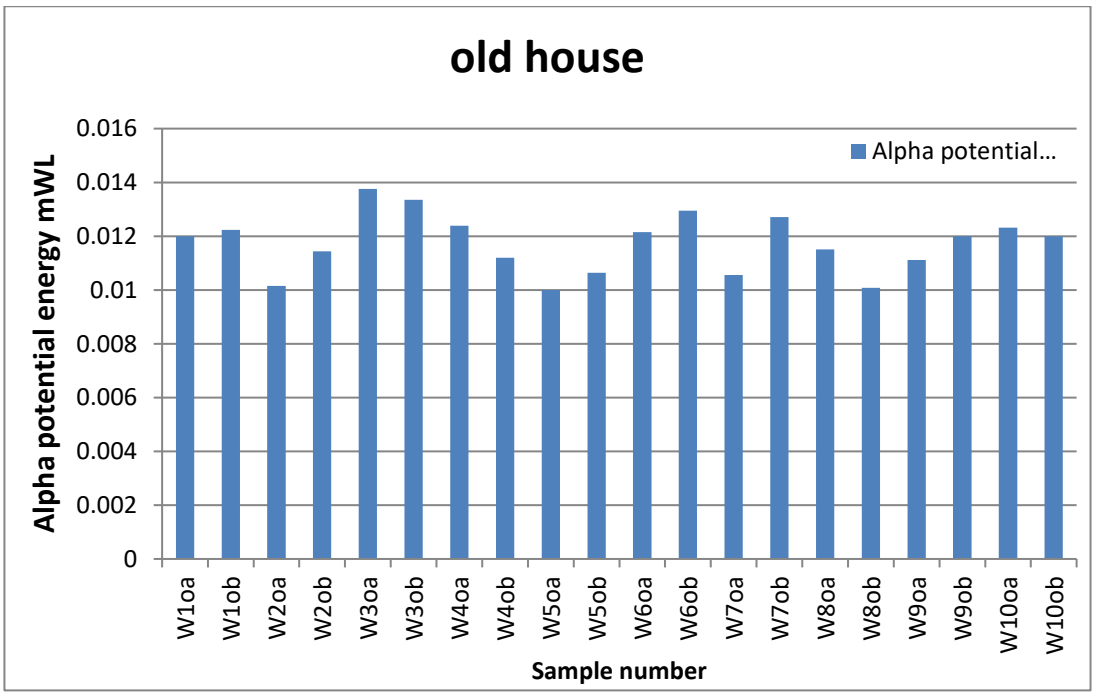

Figure 0.21. Potential alpha energy for the winter season of old houses using the CR39 nuclear trace detector.

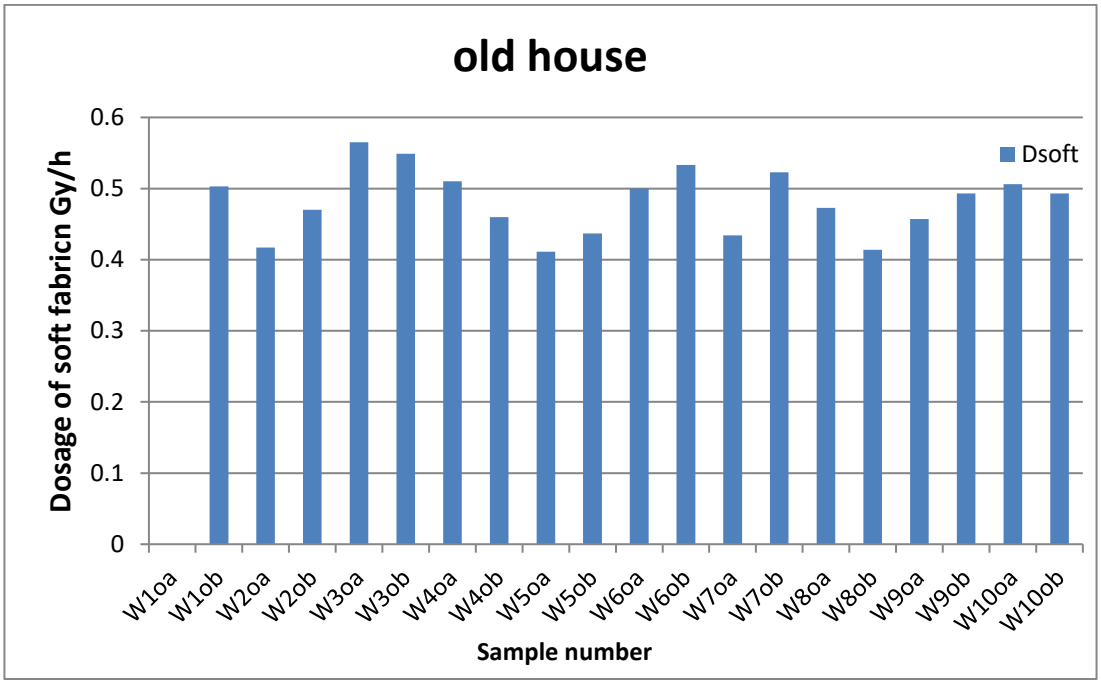

Figure 0.22. Dosage of soft fabric for the winter season for old houses using the CR-39 nuclear trace detector.

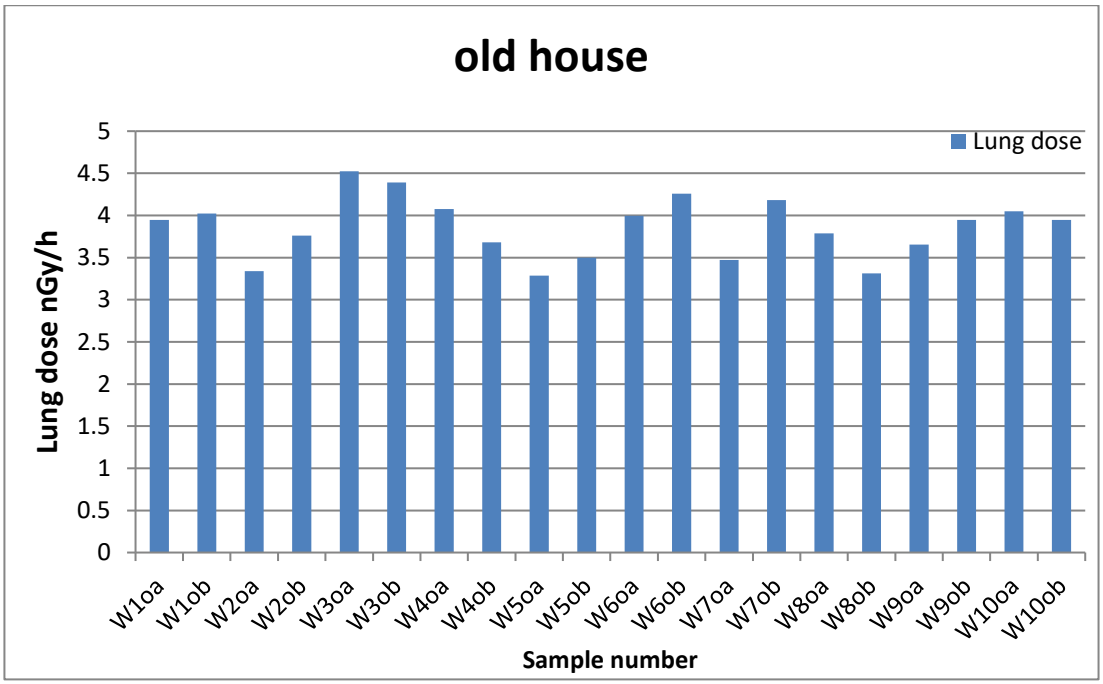

Figure 0.23. Dose to the lung for the winter season for old houses, using the CR-39 nuclear trace detector.

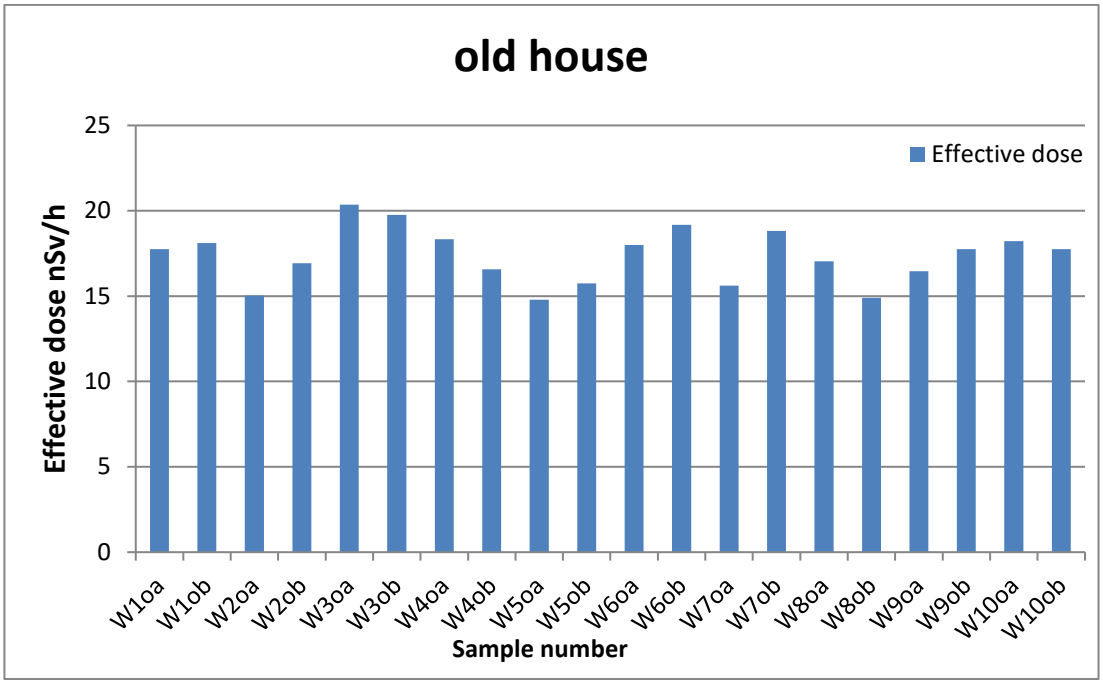

Figure 5.24. The effective dose for the winter season of old houses using the CR-39 nuclear trace detector.

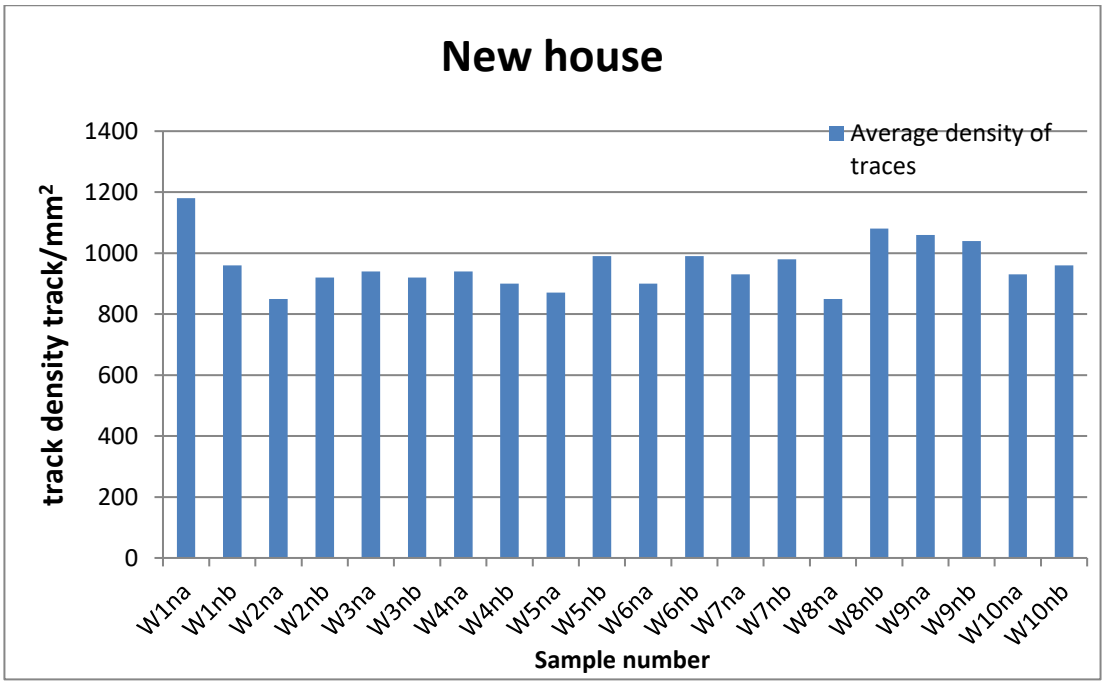

Figure 0.25. Average trace density of radon gas for the winter season for new houses using the CR-39 nuclear trace detector.

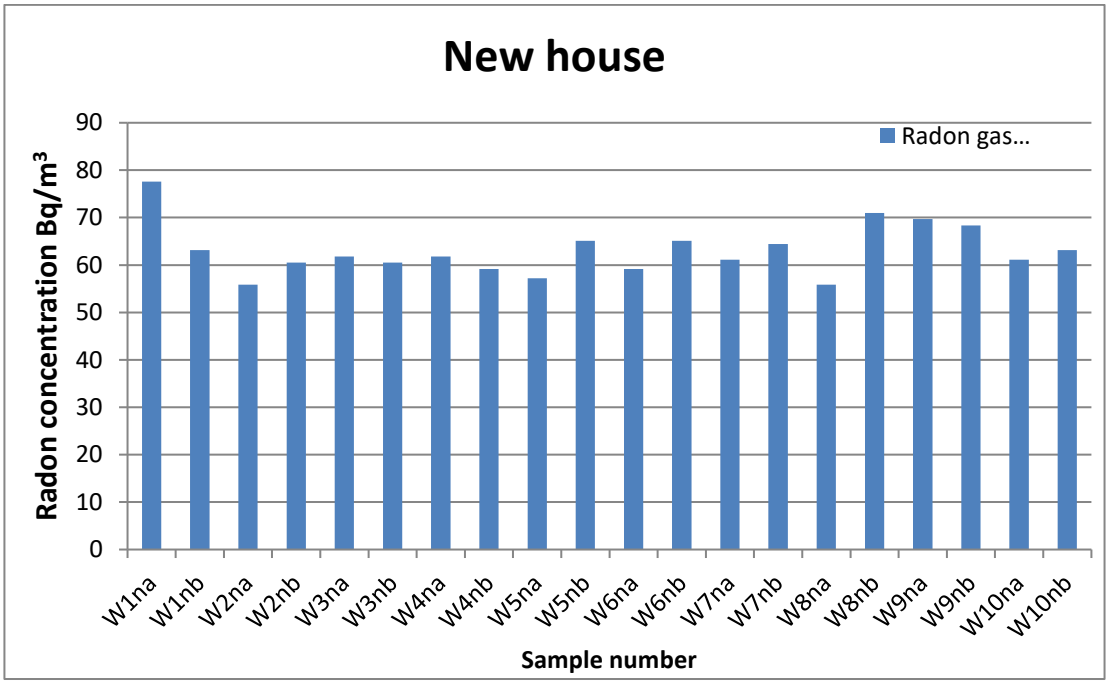

Figure 0.26. Levels of radon gas concentrations for the winter season for new houses using the CR-39 nuclear trace detector.

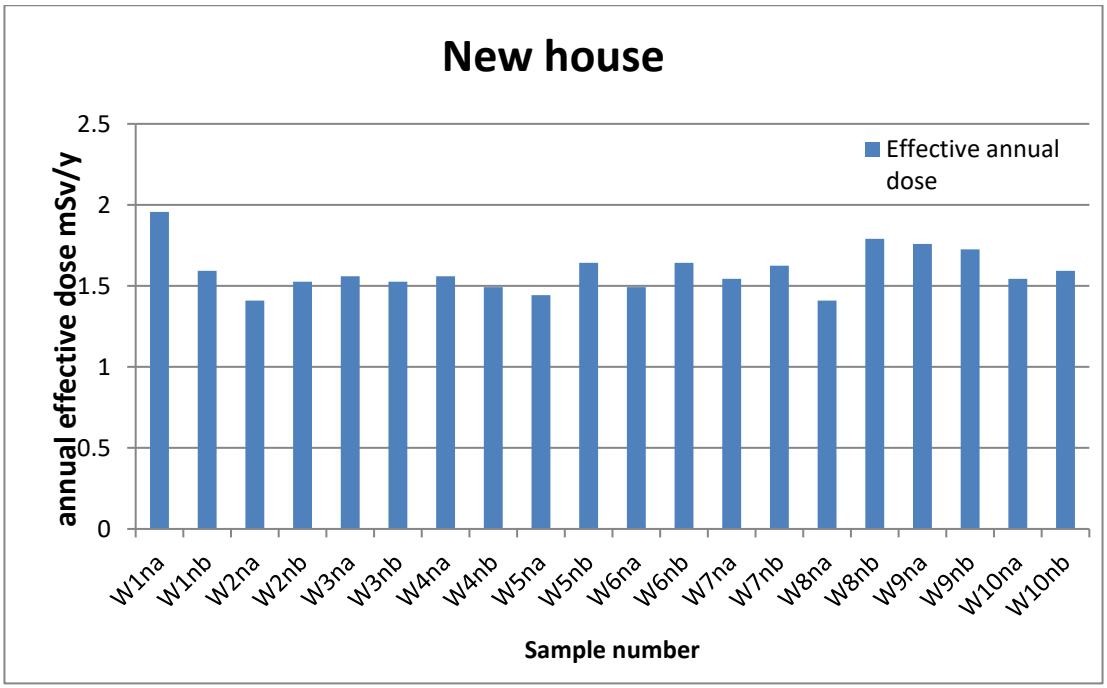

Figure 5.27. The annual effective dose for the winter season of new houses using the CR-39 nuclear trace detector.

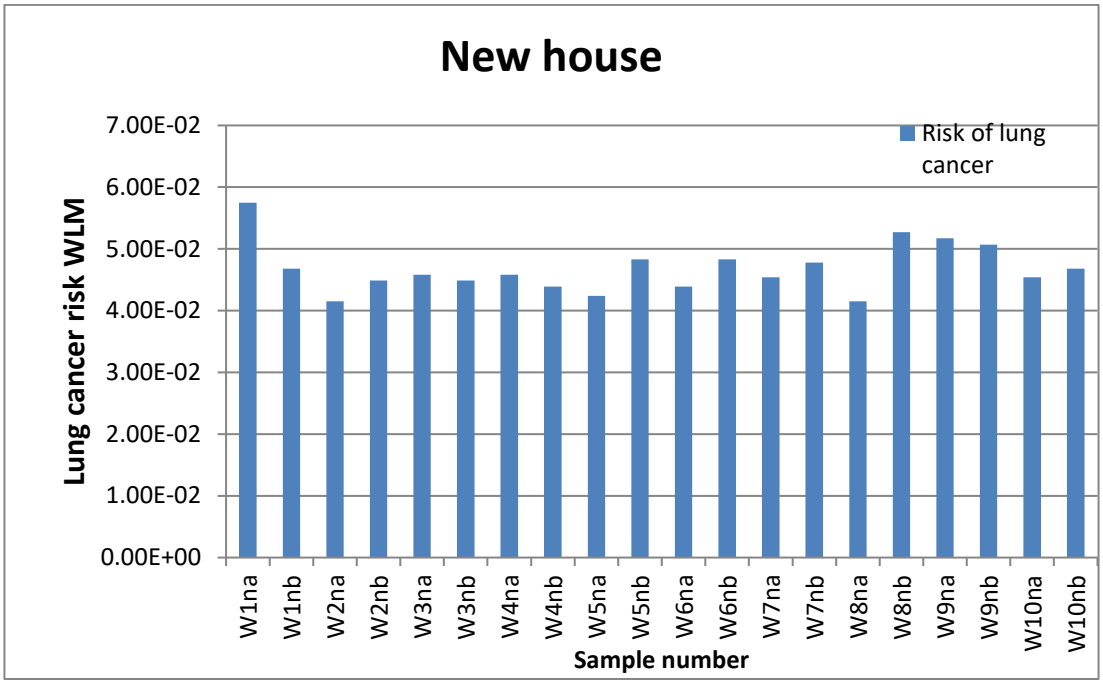

Figure 5.28. Risk of lung cancer for the winter season for new houses using the CR39 nuclear trace detector.

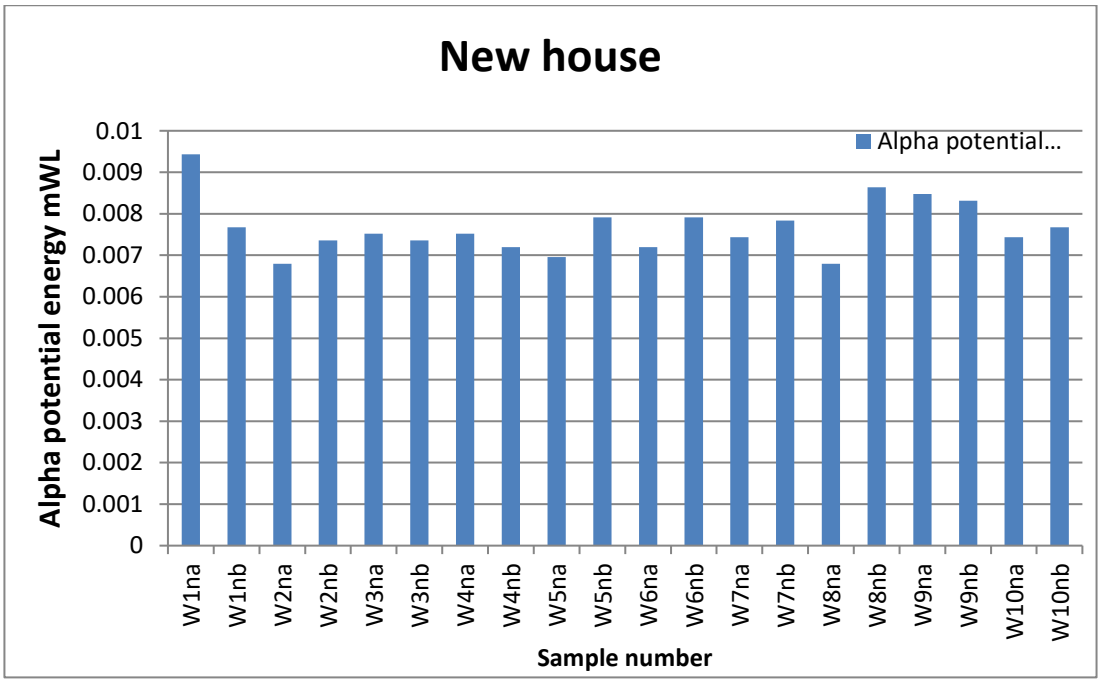

Figure 0.29. Potential alpha energy for the winter season of new houses using the CR39 nuclear trace detector.

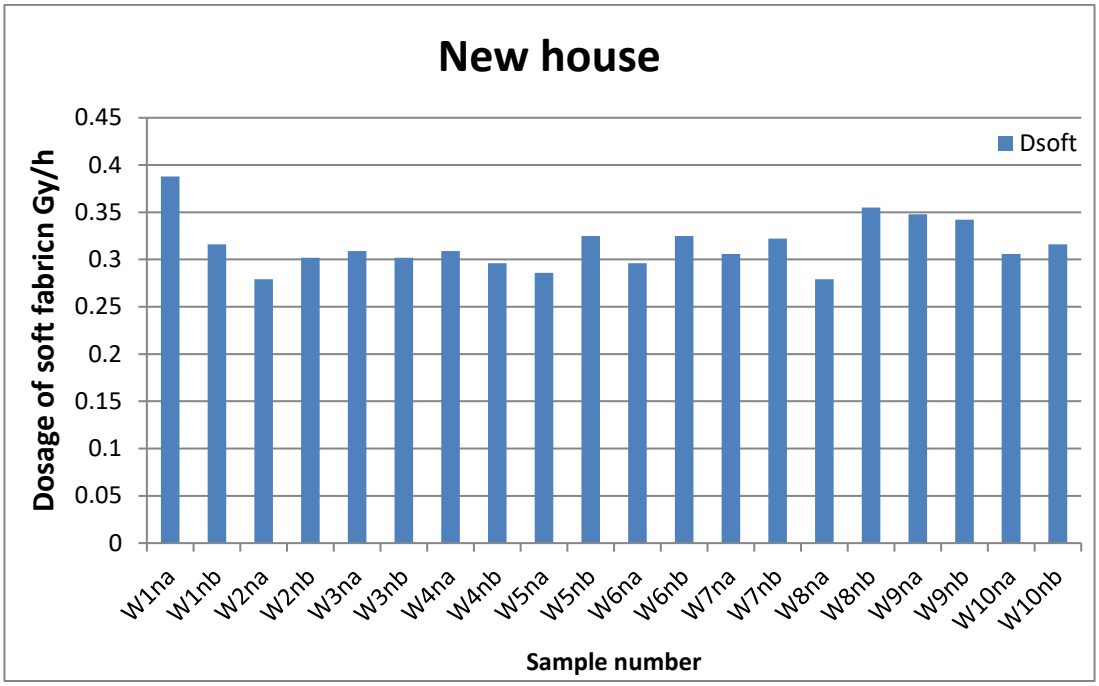

Figure 5.30. Dosage of soft fabric for the winter season for new houses using the CR-39 nuclear trace detector.

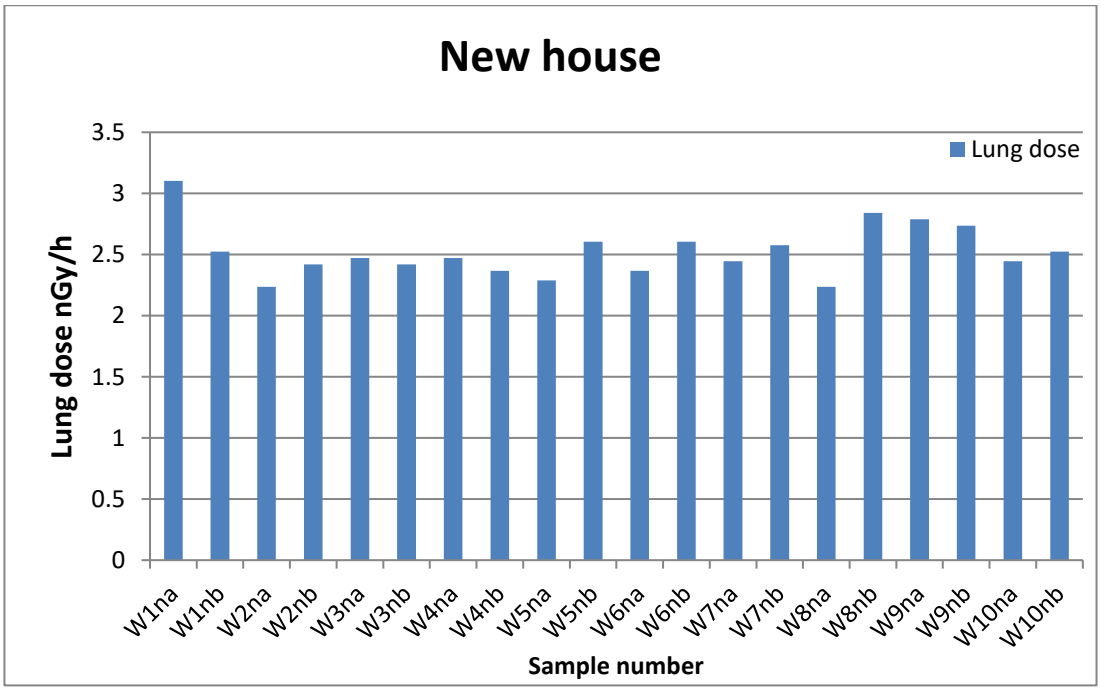

Figure 0.31. Dose to the lung for the winter season for new houses, using the CR-39 nuclear trace detector.

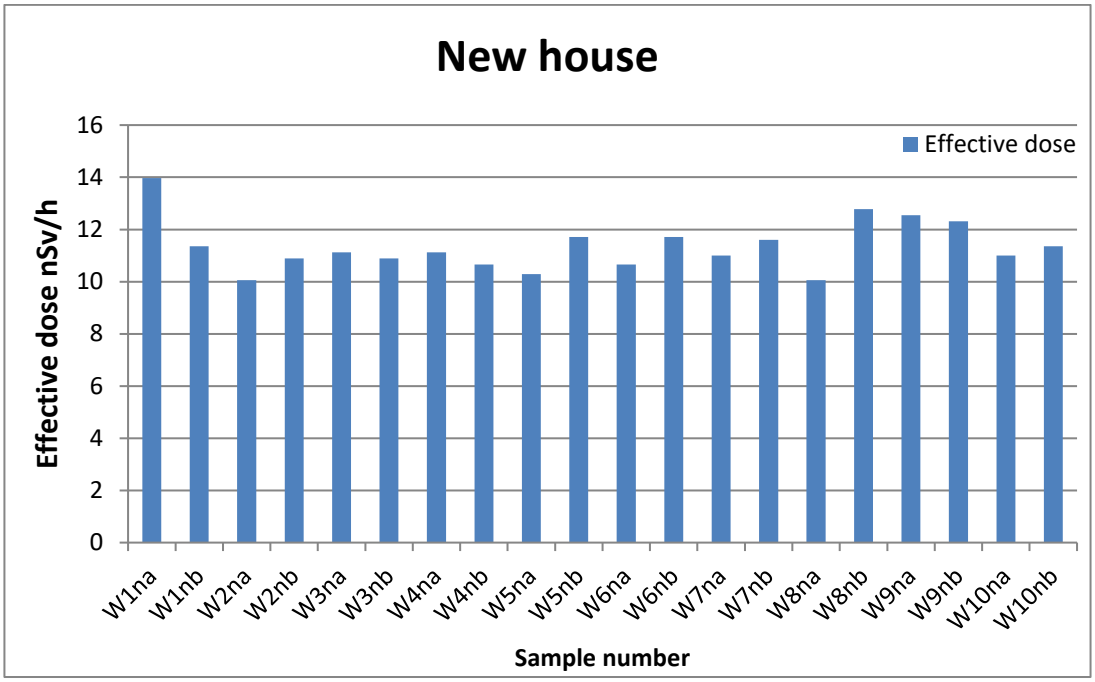

Figure 0.32. The effective dose for the winter season of new houses using the CR-39 nuclear trace detector.

Table 5.5. Some important local studies in Türkiye.

Area	**Mean concentration of radon Bq/m3**	**Reference**	**Author**	**Year**
İzmir -Dikili geothermal area	114	110	Y. Yarar	2006
Sivas	120	104	Mihci, M et al.	2010
Artvin and Ardahan provinces	21-321 & 53-736	109	B. Kucukomeroglu et al.	2011
Samsun province	106	111	B. Kucukomeroglu et al.	2012
81 province	81	105	N. Celebi et.al.	2014
Karabuk (average)	60-92 at winter 37-51 at summer	Present work	2022	

Table 5.6. Average radon concentrations in some countries.

No.	Country	Average Radon Concentration (Bq/m^3)	Reference
1	**Cyprus**	7	(115)
2	**Greece**	73	(116)
3	**Italy**	75	(117)
4	**France**	62	(118)
5	**Hungary**	107	(119)
6	**Iran**	82	(120)
7	**Syria**	10	(121)
8	**Pakistan**	30	(122)
9	**Egypt**	9	(123)
10	**UNSCEAR**	**Median** 46	(8)

PART 6

CONCLUSIONS

Through the results obtained, we conclude that the concentrations of radon gas inside the old dwellings in Karabük province were more than the modern ones. This is due to the nature of the building materials used and the style of construction (where we find glass facades that occupy larger spaces in modern homes), and some building were small with bad ventilation

These results agreed with the results of local studies, such as the study of N. Celebi et al (81Bq/m^3) (2014, 2022)[105]. They were close to international studies of countries neighboring Turkey, such as Greece was (73 Bq/m^3) [116], and in Iran was (82 Bq/m^3) [120], in addition to the global average of 46 Bq/m^3 measured by UNSCEAR [8]. They were somewhat far from the results of radon concentrations on the island of Cyprus (7 Bq/m^3) [115] and in Syria(10 Bq/m^3) [121]. This difference may be due to the nature of the land, as well as the style of construction and the materials used in it.

The radioactive indices of radon gas were also calculated, and they were higher in old homes than in modern homes, but we find that they are less than the values recommended by scientific institutions. This study is an addition and update to the data available in Türkiye.

6.1. RECOMMENDATIONS AND FUTURE STUDIES

- Pay close attention to detail and work with the ventilation system, particularly in older buildings. Seal all floor and wall cracks before painting since the majority of radon gas emissions originate in the earth, using the right materials and adopting construction techniques that provide resilience to weather changes also recommended.

- A larger and more thorough investigation of the Karabük site, including a look at how parameters such as ventilation and humidity affect the radon concentrations.
- Fresh measurements with the (Alpha GUARD) gadget and the most recent techniques
- One of the newest gadgets, it can also record radon levels under different environmental circumstances.
- Regularly measuring radon levels, particularly in enclosed spaces and underground storage
- Analyzing the amount of radon present in soil and water, which are radon's primary sources.

REFERENCES

[1] D. York and R. M. Farquhar, *The earth's age and geochronology*. Elsevier, 2013.

[2] R. E. White, *Introduction to the principles and practice of soil science.*, no. Second Edition. Blackwell Scientific Publications, 1987.

[3] A. Abbady, A. M. El-Arabi, A. E. Abbady, and S. Taha, "Gamma-ray measurements of natural radioactivity in cultivated and reclaimed soil, Upper Egypt," 2007.

[4] A. S. Al-Saif, "Radioecological aspects of hail region: behavior of some radionuclides in soil," *M. Sc, King Saud University*, 2009.

[5] L. L. Thatcher, V. J. Janzer, and K. W. Edwards, *Methods for determination of radioactive substances in water and fluvial sediments*. US Government Printing Office, 1977.

[6] P. Slovic, "The perception gap: Radiation and risk," *Bulletin of the atomic scientists*, vol. 68, no. 3, pp. 67–75, 2012.

[7] R. Hedvall and B. Erlandsson, "Radioactivity concentrations in non-nuclear industries," *J Environ Radioact*, vol. 32, no. 1–2, pp. 19–31, 1996.

[8] I. V Yarmoshenko, A. A. Ekidin, M. V Zhukovsky, and A. D. Onischenko, "Identification of technogenic contamination by natural radionuclides," in *Naturally occurring radioactive material (NORM V). Proceedings of an international symposium. Posters*, 2008.

[9] U. N. S. C. on the E. of A. Radiation, "Effects of ionizing radiation," *Scientific Annexes E*, pp. 203–204, 2008.

[10] M. Charles, "UNSCEAR Report 2000: sources and effects of ionizing radiation." 2001.

[11] K.-H. Ng, "Non-ionizing radiations–sources, biological effects, emissions and exposures," in *Proceedings of the international conference on non-ionizing radiation at UNITEN*, sn, 2003, pp. 1–16.

[12] G. J. Weir Jr, "Chemical Protection of the Body Against Ionizing Radiation." JSTOR, 1965.

[13] G. Sgouros, "Alpha-particles for targeted therapy," *Adv Drug Deliv Rev*, vol. 60, no. 12, pp. 1402–1406, 2008.

[14] A. Ishimaru, *Electromagnetic wave propagation, radiation, and scattering: from fundamentals to applications*. John Wiley & Sons, 2017.

[15] Y. Kanada-En'yo, M. Kimura, and H. Horiuchi, "Cluster structure in stable and unstable nuclei," *The European Physical Journal A-Hadrons and Nuclei*, vol. 25, pp. 305–310, 2005.

[16] J. Peterson, M. MacDonell, L. Haroun, F. Monette, R. D. Hildebrand, and A. Taboas, "Radiological and chemical fact sheets to support health risk analyses for contaminated areas," *Argonne National Laboratory Environmental Science Division*, vol. 133, pp. 40–41, 2007.

[17] U. N. S. C. on the E. of A. Radiation, "Effects of ionizing radiation," *Scientific Annexes E*, pp. 203–204, 2008.

[18] A. Hameed Al-Mashhadani, H. Saddi Ali, K. Sameen Ali, A. H. Al-Mashhadani, and K. Sameen Ali Study, "of Radiation Pollution of Groundwater in Al-Tuz, Salah Al-Din Governorate," *Iraq. World Journal of Applied Physics*, vol. 2, no. 3, pp. 85–91, 2017, doi: 10.11648/j.wjap.20170203.14.

[19] Q. M. Rashed-Nizam *et al.*, "Radiological risk analysis of sediment from Kutubdia island, Bangladesh due to natural and anthropogenic radionuclides," *International Journal of Radiation Research*, vol. 14, no. 4, pp. 373–377, Oct. 2016, doi: 10.18869/acadpub.ijrr.14.4.373.

[20] J. Lilley, *Nuclear physics: principles and applications*. John Wiley & Sons, 2013.

[21] D. J. Strom, "Health impacts from acute radiation exposure," 2003.

[22] G. Kaur, S. J. Singh Bajwa, and G. Kaur, "Radiation hazards in operation theatre: Anaesthesiologist's concerns and preventive strategies," *Indian Journal of Anaesthesia*, vol. 59, no. 7. Indian Society of Anaesthetists, pp. 455–456, Jul. 16, 2015. doi: 10.4103/0019-5049.160970.

[23] E. M. Köksal *et al.*, "A survey of 222 Rn concentrations in dwellings of Turkey," *J Radioanal Nucl Chem*, vol. 259, pp. 213–216, 2004.

[24] A. Sroor, S. M. El-Bahi, F. Ahmed, and A. S. Abdel-Haleem, "Natural radioactivity and radon exhalation rate of soil in southern Egypt," *Applied Radiation and Isotopes*, vol. 55, no. 6, pp. 873–879, 2001.

[25] M. Karpińska, S. Wołkowicz, Z. Mnich, M. Zalewski, K. Mamont-Cieśla, and J. Kapała, "Comparative studies of health hazard from radon (Rn-222) in two selected lithologic formations in the Suwałki region (in Poland)," *J Environ Radioact*, vol. 61, no. 2, pp. 149–158, 2002.

[26] S. Tokonami *et al.*, "Radon and thoron exposures for cave residents in Shanxi and Shaanxi provinces," *Radiat Res*, vol. 162, no. 4, pp. 390–396, 2004.

[27] C. Sainz, A. Dinu, T. Dicu, K. Szacsvai, C. Cosma, and L. S. Quindós, "Comparative risk assessment of residential radon exposures in two radon-prone

areas, Ştei (Romania) and Torrelodones (Spain)," *Science of the Total Environment*, vol. 407, no. 15, pp. 4452–4460, 2009.

[28] C. Nemeth, V. Jobbagy, N. Kavasi, J. Somlai, T. Kovacs, and S. Tokonami, "Radon and thoron parallel measurements in dwellings nearby a closed Hungarian uranium mine," *nukleonika*, vol. 55, no. 4, pp. 459–462, 2010.

[29] R. I. Obed, A. K. Ademola, M. Vascotto, and G. Giannini, "Radon measurements by nuclear track detectors in secondary schools in Oke-Ogun region, Nigeria," *J Environ Radioact*, vol. 102, no. 11, pp. 1012–1017, 2011.

[30] J. Madureira, I. Paciência, J. Rufo, A. Moreira, E. de Oliveira Fernandes, and A. Pereira, "Radon in indoor air of primary schools: determinant factors, their variability and effective dose," *Environ Geochem Health*, vol. 38, pp. 523–533, 2016.

[31] A. S. Silva and M. L. Dinis, "Indoor radon levels and total gamma dose rates measurements in Portuguese thermal spas," *International Journal of Occupational and Environmental Safety*, vol. 1, no. 1, pp. 79–87, 2017.

[32] د. ه. إ. الخطيبand د. ا. ل. والتوزيع, *مبادئ الاشعاع والوقاية الاشعاعية*. 2019. [Online]. Available: https://books.google.iq/books?id=LbAREAAAQBAJ

[33] G. F. Knoll, *Radiation detection and measurement*. John Wiley & Sons, 2010.

[34] J. R. Stetter and J. Li, "Amperometric gas sensors a review," *Chem Rev*, vol. 108, no. 2, pp. 352–366, 2008.

[35] S. A. Durrani and R. K. Bull, *Solid state nuclear track detection: principles, methods and applications*, vol. 111. Elsevier, 2013.

[36] S. A. Durrani, "The use of solid-state nuclear track detectors in radiation dosimetry, medicine and biology," *Nuclear Tracks and Radiation Measurements (1982)*, vol. 6, no. 4, pp. 209–228, 1982.

[37] D. A. Young, "Etching of radiation damage in lithium fluoride," *Nature*, vol. 182, 1958.

[38] S. A. Durrani, "Nuclear tracks: A success story of the 20th century," *Radiat Meas*, vol. 34, no. 1–6, pp. 5–13, 2001.

[39] S. A. Durrani and R. Ilic, *Radon measurements by etched track detectors-applications in radiation protection, earth sciences*. World Scientific, 1997.

[40] M. F. L'Annunziata, *Handbook of radioactivity analysis*. Academic press, 2012.

[41] R. L. Fleischer, P. B. Price, and R. M. Walker, *Nuclear tracks in solids: principles and applications*. Univ of California Press, 2022.

[42] S. A. Durrani and R. K. Bull, *Solid state nuclear track detection: principles, methods and applications*, vol. 111. Elsevier, 2013.

[43] M. A. Kenawy and A. M. Sayed, “Comparison of Various Types of SSNTD for neutron Dosimetry,” in *Solid State Nuclear Track Detectors*, Elsevier, 1980, pp. 559–571.

[44] U. L. F. Gedde, *Polymer physics*. Springer Science & Business Media, 1995.

[45] A. Waheed, S. Manzoor, R. Cherubini, G. Moschini, L. Lembo, and H. A. Khan, “A more suitable etching condition to register low energy proton tracks in CR39 for neutron dosimetry,” *Nucl Instrum Methods Phys Res B*, vol. 47, no. 3, pp. 320–328, 1990.

[46] R. J. Tanner, D. J. Thomas, D. T. Bartlett, and N. Horwood, “Systematic errors in the readings of track etch neutron dosemeters caused by the energy dependence of response,” *Radiat Meas*, vol. 31, no. 1–6, pp. 483–486, 1999.

[47] R. M. Cassou and E. V Benton, “Properties and applications of CR-39 polymeric nuclear track detector,” *Nuclear Track Detection*, vol. 2, no. 3, pp. 173–179, 1978.

[48] T. Yamauchi, A. El-Rahmany, D. Mineyama, H. Nakai, and K. Oda, “Surface layer in CR-39 plastic track detector where the bulk etch rate is enhanced,” *Radiat Meas*, vol. 37, no. 2, pp. 119–125, 2003.

[49] P. K. Diwan, V. Sharma, S. K. Sharma, and S. Kumar, “Registration temperature effect on sensitivity of CR-39 (DOP) and SR-90 polymer track detectors,” *Radiat Meas*, vol. 36, no. 1–6, pp. 89–92, 2003.

[50] G. Espinosa, R. V Griffith, L. Tommasino, S. A. Durrani, and E. V Benton, “Solid State Nuclear Track Detectors,” *Nucl. Tracks and Radiation Measurements (Pergamon, Oxford, 1984)*, vol. 8, p. 289, 1984.

[51] G. Etiope and G. Martinelli, “Migration of carrier and trace gases in the geosphere: an overview,” *Physics of the earth and planetary interiors*, vol. 129, no. 3–4, pp. 185–204, 2002.

[52] A. C. George, “World history of radon research and measurement from the early 1900’s to today,” in *AIP Conference Proceedings*, American Institute of Physics, 2008, pp. 20–33.

[53] J. K. Otton, L. C. S. Gunderson, and R. R. Schumann, “The geology of radon: US Geological Survey,” *General Interest Publication*, p. 28, 1992.

[54] S. A. Owusu and M. E. K. T. Addison, “DETERMINATION OF THE RADON CONCENTRATION IN UNDERGROUND WATER IN SELECTED AREAS IN AND AROUND KUMASI,” 2012.

[55] U. States. E. P. Agency. O. of R. Programs, *Final environmental impact statement for standards for the control of byproduct materials from uranium ore processing (40 CFR 192).*, vol. 83. Office of Radiation Programs, US Environmental Protcetion Agency, 1983.

[56] A. C. Chamberlain and E. D. Dyson, “The dose to the trachea and bronchi from the decay products of radon and thoron,” *Br J Radiol*, vol. 29, no. 342, pp. 317–325, 1956.

[57] L. Oufni, N. Manaut, S. Taj, and B. Manaut, “Determination of radon and thoron concentrations in different parts of some plants used in traditional medicine using nuclear track detectors,” *American journal of environmental protection*, vol. 1, no. 2, pp. 34–40, 2013.

[58] H. S. Virk and B. Singh, “Radon anomalies in soil-gas and groundwater as earthquake precursor phenomena,” *Tectonophysics*, vol. 227, no. 1–4, pp. 215–224, 1993.

[59] S. A. Durrani and R. Ilic, *Radon measurements by etched track detectors-applications in radiation protection, earth sciences*. World Scientific, 1997.

[60] J. K. Otton, L. C. S. Gunderson, and R. R. Schumann, “The geology of radon: US Geological Survey,” *General Interest Publication*, p. 28, 1992.

[61] J. K. Otton, L. C. S. Gundersen, and R. R. Schumann, “The Geology of Radon. US Department of the Interior,” *US Geological Survey, Open Report*, vol. 30, 1992.

[62] P. de Jong, *Exposure to natural radioactivity in the Netherlands: the impact of building materials*. University Library Groningen][Host], 2010.

[63] G. Faure, “Isotope systematics in two-component mixtures,” *Principles of isotope geology*, pp. 141–153, 1986.

[64] L. A. Najam, N. F. Tawfiq, and R. H. Mahmood, “Radon Concentration in Some Building Materials in Iraq Using CR-39 Track Detector,” *International Journal of Physics*, vol. 1, no. 3, pp. 73–76, 2013, doi: 10.12691/ijp-1-3-3.

[65] A. Bashir, K. Kudo, and X. Yang, “Radon measurements in some houses of Tsukuba science city, Japan,” *Nucl Tracks Radiat Meas*, vol. 22, no. 1–4, pp. 395–398, 1993.

[66] W. W. Nazaroff and A. V Nero, “Radon and its decay products in indoor air,” 1988.

[67] J. H. Lubin *et al.*, “Risk of lung cancer and residential radon in China: pooled results of two studies,” *Int J Cancer*, vol. 109, no. 1, pp. 132–137, 2004.

[68] W. H. Organization, *WHO handbook on indoor radon: a public health perspective*. World Health Organization, 2009.

[69] J.-F. Lecomte *et al.*, “ICRP publication 126: radiological protection against radon exposure,” *Ann ICRP*, vol. 43, no. 3, pp. 5–73, 2014.

[70] J. Miles, “Development of maps of radon-prone areas using radon measurements in houses,” *J Hazard Mater*, vol. 61, no. 1–3, pp. 53–58, 1998.

[71] A. Azam, A. H. Naqvi, and D. S. Srivastava, “Radium concentration and radon exhalation measurements using LR-115 type II plastic track detectors,” *Nuclear geophysics*, vol. 9, no. 6, pp. 653–657, 1995.

[72] P. C. Kalsi, A. Ramaswami, and V. K. Manchanda, “Solid state nuclear track detectors and their applications,” *BARC Newsletter*, vol. 257, pp. 6–15, 2005.

[73] M. F. Zaki, T. M. Hegazy, U. Seddik, and A. Morsy, “Variation of the track etch rates of alpha-particle trajectory in PADC,” *Radiation Effects and Defects in Solids*, vol. 160, pp. 53–58, 2005, [Online]. Available: https://api.semanticscholar.org/CorpusID:96637094

[74] S. Manzoor *et al.*, “Nuclear track detectors for environmental studies and radiation monitoring,” *Nuclear Physics B-Proceedings Supplements*, vol. 172, pp. 92–96, 2007.

[75] M. Lang, R. Devanathan, M. Toulemonde, and C. Trautmann, “Advances in understanding of swift heavy-ion tracks in complex ceramics,” *Curr Opin Solid State Mater Sci*, vol. 19, no. 1, pp. 39–48, 2015.

[76] F. Spurný and K. Turek, “Neutron dosimetry with solid state nuclear track detectors,” *Nuclear Track Detection*, vol. 1, no. 3–4, pp. 189–197, 1977.

[77] S. A. Durrani and R. K. Bull, *Solid state nuclear track detection: principles, methods and applications*, vol. 111. Elsevier, 2013.

[78] K. Hareesh, G. Sanjeev, A. K. Pandey, and V. Rao, “Characterization of UV-irradiated Lexan polycarbonate films,” *Iranian polymer journal*, vol. 22, no. 5, pp. 341–349, 2013.

[79] M. Dheyaa, A. Ridha, N. Kadhim, and A. El-Taher, “Effects of Changing the Exposure Time of CR-39 Detector to Alpha Particles on Etching Conditions,” Aug. 2020, doi: 10.18576/jrna/050206.

[80] S. C. Sarkar, I. Ali, D. Paul, M. R. Bhuiyan, and S. M. A. Islam, “Measurement of natural and artificial radioactivity in soil at some selected Thanas around the TRIGA Mark-II research reactor at AERE, Savar, Dhaka,” *J Environ Prot (Irvine, Calif)*, vol. 2, no. 10, p. 1353, 2011.

[81] B. Dörschel, D. Hermsdorf, and U. Reichelt, “Experimental determination of the critical angle for particle registration and comparison with model predictions,” *Radiat Meas*, vol. 35, no. 3, pp. 189–193, 2002.

[82] P. C. Kalsi, A. Ramaswami, and V. K. Manchanda, “Solid state nuclear track detectors and their applications,” *BARC Newsletter*, vol. 257, pp. 6–15, 2005.

[83] M. Mihci, A. Buyuksarac, A. Aydemir, and N. Celebi, “Indoor and outdoor Radon concentration measurements in Sivas, Turkey, in comparison with geological setting,” *J Environ Radioact*, vol. 101, no. 11, pp. 952–957, 2010.

[84] N. Celebi, B. Ataksor, H. Taskın, and N. A. Bingoldag, “Indoor radon measurements in Turkey dwellings,” *Radiat Prot Dosimetry*, vol. 167, no. 4, pp. 626–632, 2015.

[85] H. Vanmarcke, “UNsCEAR 2000: sources of ionizing radiation,” *Annalen van de Belgische vereniging voor stralingsbescherming*, vol. 27, no. 2, pp. 41–65, 2002.

[86] H. Zeeb, F. Shannoun, and W. H. Organization, *WHO handbook on indoor radon: a public health perspective*. World Health Organization, 2009.

[108] Turkish Atomic Energy Authority.”Regulations for the radiation safety, Official Journal, Date/Number: 24.03. 2000. [109] B. Kucukomeroglu, Y. O. Yesilbag, A. Kurnaz, N. Celik, U. Cevik, and N. Celebi, Radiological characterisation of Artvin and Ardahan provinces of Turkey, Radiation Protection Dosimetry, vol. 145, no. 4, pp. 389-394, 2011.

[110] Yarar, T. Günaydi and N. Çelebi, Determination of radon concentrations of the Dikili geothermal area in western Turkey, Radiation Protection Dosimetry, vol. 118, no. 1, pp. 78-81, 2006.

[111] B. Kucukomeroglu, F. Maksutoglu, N. Damla, U. Cevik and N. Celebi, A study of environmental radioactivity measurements in the Samsun province, Turkey, Radiation Protection Dosimetry, vol. 152, no. 4, pp. 369-375, 2012.

[112] International Commission on Radiological Protection (ICRP),”Protection against Radon-222 at home and at work,” PERGAMON, publishing 65,volume 2,No.2,1993.

[113] S. Kansal, R. Mehra and N. P. Singh, “Life time fatality risk assessment due to variation of indoor radon concentration in dwellings in western Haryana”,Applied Radiation and Isotopes, vol. 70, no. 7,pp. 1110-1112, 2012.

[114] International Commission on Radiological Protection (ICRP), “Statement on Radon”, 2009.

[115] Christofides, S. and G. Christodoulides. 1993 Airborne 222Rnconcentration in Cypriot houses. Health Phys. 64(4): 392-396 .

[116] Georgiou, E. Ntalles, K. Molfetas, M. Athanassiadis, A. Proukakis, C., “Radon measurements in Greece”, Radiation Protection Practice. Proceedings of the 7th International Congress of the International Radiation Protection Association (V-1). Pergamon Press, Sydney. INIS,V20,N13,1988.

[117] De Bortoli, M. and P. Gaglione;” 226Ra in environmental materials and foods”. Health Phys. 22:43-48. 1972.

[118] Rannou, A. and G. Tymen. “Lesresultats des campagnesdemesures de radon etfacteursexplicatifs”. Exposition au Radon dans les Habitations – Aspects Technique et Sanitaires. SFRP, Paris. p. 42-63 ,1989.

[119] Nikl, I. “The radon concentration and absorbed dose rate in Hungarian dwellings”. Radiat. Prot. Dosim. 67(3): 225-228, 1996.

[120] Sohrabi, M. and Solaymanian A.R., Indoor radon level measurements in Iran using AEOI passive dosimeters. Radiation Protection Practice. Proceedings of the 7th International Congress of the International Radiation Protection Association (V-1) Pergamum Press, Sydney. p. 242-245, 1988.

[121] Bem, H. Domanski, T. Bakir, Y.Y. Al-Zenki S.,”Radon survey in Kuwait houses. IRPA9, 1996 International Congress on Radiation Protection. Proceedings, Volume 2. IRPA,Vienna. p. 101-103,1996.

[122] Tufail M., Amin M., Akhtar W., Khan H.A., Qureshi A.A., Manzoor S., “Radon concentration in some houses of Islamabad and Rawalpindi”, Pakistan. Nucl. Tracks Radiat. Meas. 19: 429-430. 1991.

[123] Kenawy, M.A. and Morsy A.A.,”Measurements of environmental 222Rn concentration in indoors and outdoors in Egypt”. Nucl. Tracks Radiat. Meas. 19: 343-345.1991

RESUME

Abdul Rahman Ahmed Mustafa AL-AJILI completed his primary and secondary education in Tikrit. He graduated from Al-Hadara High School for Boys. He began his education at Tikrit University, College of Education for Pure Sciences, Department of Physics in 2015 and graduated in 2019. He began working as a teacher in 2019 at the Iraq Middle School for Boys for two years, after which he moved to Al-Maqasid Secondary School for Boys. He completed the master's program that began in the Physics Department in the year 2021. At Karabuk University, Institute of Science, Department of Physics. He began working in the Ministry of Education as a physics teacher in 2021 and is still working in the same place.